Journal of Medicinal Chemistry Article

J. Med. Chem. **2010,** *53,* 8569–8584 **8569**
DOI: 10.1021/jm101115u

Synthesis and Evaluation of Azetidinone Analogues of Combretastatin A-4 as Tubulin Targeting Agents

Niamh M. O'Boyle,[†] Miriam Carr,[†] Lisa M. Greene,[‡] Orla Bergin,[§] Seema M. Nathwani,[‡] Thomas McCabe,[∥] David G. Lloyd,[⊥] Daniela M Zisterer,[‡] and Mary J. Meegan*[,†]

[†]*School of Pharmacy and Pharmaceutical Sciences, Centre for Synthesis and Chemical Biology, Trinity College Dublin, Dublin 2, Ireland,* [‡]*School of Biochemistry and Immunology, Trinity College Dublin, Dublin 2, Ireland,* [§]*UCD Conway Institute and School of Biomolecular and Biomedical Science, University College Dublin, Belfield, Dublin 4, Ireland,* [∥]*School of Chemistry, Trinity College Dublin, Dublin 2, Ireland, and* [⊥]*Molecular Design Group, School of Biochemistry and Immunology, Trinity College Dublin, Dublin 2, Ireland*

Received August 27, 2010

The synthesis and antiproliferative activity of a new series of rigid analogues of combretastatin A-4 are described which contain the 1,4-diaryl-2-azetidinone (β-lactam) ring system in place of the usual ethylene bridge present in the natural combretastatin stilbene products. These novel compounds are also substituted at position 3 of the β-lactam ring with an aryl ring. A number of analogues showed potent nanomolar activity in human MCF-7 and MDA-MB-231 breast cancer cell lines, displayed in vitro inhibition of tubulin polymerization, and did not cause significant cytotoxicity in normal murine breast epithelial cells. 4-(4-Methoxyaryl)-substituted compound **32**, 4-(3-hydroxy-4-methoxyaryl)-substituted compounds **35** and **41**, and the 3-(4-aminoaryl)-substituted compounds **46** and **47** displayed the most potent antiproliferative activity of the series. β-Lactam **41** in particular showed subnanomolar activity in MCF-7 breast cancer cells (IC_{50} = 0.8 nM) together with significant in vitro inhibition of tubulin polymerization and has been selected for further biochemical assessment. These novel β-lactam compounds are identified as potentially useful scaffolds for the further development of antitumor agents that target tubulin.

Introduction

Microtubules are cytoskeletal structures that are formed by self-assembly of α and β tubulin heterodimers and are involved in many cellular functions.[1] Their most important role is in the formation of the mitotic spindle, and they are essential to the mitotic division of cells. Tubulin is an α,β heterodimeric protein that is the main constituent of microtubules. Tubulin is the target of numerous small molecule antiproliferative ligands that act by interfering with microtubule dynamics.[2] These ligands can be broadly divided into two categories: those that inhibit the formation of the mitotic spindle such as colchicine (**1**, Figure 1)[3,4] and vinblastine[5] and those that inhibit the disassembly of the mitotic spindle once it has formed, such as paclitaxel.[6] The three characterized binding sites of tubulin are the taxane domain, the vinca domain, and the colchicine domain, and many compounds interact with tubulin at these known sites. Many tubulin binding compounds, such as paclitaxel and vinblastine, are in clinical use for various types of cancer.[2] Antimitotic agents are one of the major classes of cytotoxic drug for cancer treatment, and microtubules are a significant target for many natural product anticancer agents such as combretastatin A-4 (**2a**, Figure 1)[7] and podophyllotoxin (**4**, Figure 1).[2,8]

The combretastatins are a group of diarylstilbenes isolated from the stem wood of the South African tree *Combretum caffrum*.[9] **2a** was found to have potent anticancer activity against a number of human cancer cell lines including multidrug resistant cancer cell lines and binds to the colchicine-binding site of tubulin.[10] A water-soluble prodrug, combretastatin A-4-phosphate (**2b**, Figure 1), is now in clinical trials for thyroid cancer[11−13] and in patients with advanced cancer.[14] **2b** induces vascular shutdown within tumors at doses less than one-tenth of the maximum tolerated dose and without detectable morbidity, assuming a MTD[a] of 1000 mg/kg.[7] Hydrolysis in vivo by endogenous nonspecific phosphatases under physiological conditions affords **2a**.[15,16] The amino derivative of **2a** (compound **3a**) is also in clinical trials as a water-soluble amino acid prodrug (**3b**, Figure 1).[17] In contrast to colchicine, the antivascular effects of **2a** in vivo are apparent well below the maximum tolerated dose, offering a wide therapeutic window. **2a** as well as being a potent inhibitor of colchicine binding is also shown to inhibit the growth and development of blood vessels, angiogenesis.[5,18−21] The cis configuration only of **2a** is biologically active, with the trans form showing little or no activity.[22] The active cis double bond in **2a** is readily converted to the more stable trans isomer during storage or metabolism, resulting in a dramatic decrease in antitumor activity.[23,24]

Various structural modifications to **2a** have been reported including variation of the A- and B-ring substituents.[25−27] Many modifications of the B-ring result in decreased bioactivity; however, substitution of the 3′-OH with an amino group

*To whom correspondence should be addressed. Phone: +353-1-8962798. Fax: +353-1-8962793. E-mail: mmeegan@tcd.ie.

[a] Abbreviations: CA-4, combretastatin A-4; EI, electron impact; ER, estrogen receptor; GTP, guanidine triphosphate; HRMS, high resolution molecular ion determination; IC, inhibitory concentration; MTD, maximum tolerated dose; MTT, 3-(4,5-dimethylthiazol-2-yl)-2,5-diphenyltetrazolium bromide; NCI, National Cancer Institute; NMR, nuclear magnetic resonance; PBS, phosphate buffered saline; SAR, structure−activity relationship; TBAF, tetrabutylammonium fluoride; TBDMS, *tert*-butyldimethylchlorosilane; THF, tetrahydrofuran; TMCS, trimethylchlorosilane; TMS, tetramethylsilane.

Published on Web 11/16/2010

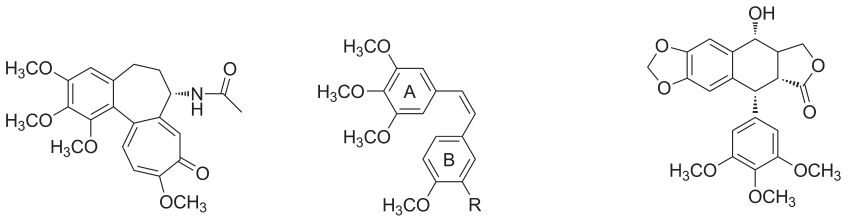

Figure 1. Colchicine (**1**), combretastatin A-4 (**2a**), related compounds **2b**, **3a**, **3b**, and podophyllotoxin (**4**).

results in potent bioactivity and good water solubility.[28] The 3,4,5-trimethoxy substituted pattern in ring A, resembling the trimethoxyaryl ring of colchicine, is optimal for bioactivity of **2a**.[24] Many conformationally restricted analogues of **2a** are known. Most of these compounds replace the cis-double bond in **2a** with a heterocyclic rigid ring scaffold structure that prevents isomerization of the cis-double bond. These analogues include the heteroarylcoumarin,[29] aroylindole,[27] imidazole,[30] 1,3-dioxolane,[31] pyrazole,[23] furazan (1,2,5-oxadiazole),[25] and benzoxepin[32] ring systems. Such nonisomerizable compounds inhibit cell growth of several human cancer cell lines, and many have been shown to be significant tubulin binding and depolymerizing effects. We now describe the synthesis and tubulin targeting activity of nonisomerizable β-lactam-containing analogues of **2a**. The anticancer activity of some β-lactam-containing compounds has been reported,[33] including the nonisomerizable combretastatin analogues containing OH and OMe substituents at C-3.[34] We have recently reported the potent antiproliferative activity of β-lactam-containing compounds that are unsubstituted at C-3 or contain methyl substituent(s) at C-3.[35] We have also reported antiproliferative and antiestrogenic activity of compounds containing the β-lactam scaffold in MCF-7 cells.[36] In continuation of our earlier work, a further panel of compounds containing the β-lactam ring were examined as potential tubulin targeting agents. These novel compounds contain an aryl-type substituent at C-3, while the rigid β-lactam ring scaffold structure allows a similar spatial arrangement between the two phenyl rings as observed in the cis conformation of **2a**.

Chemistry

The synthesis of the target β-lactams is illustrated in Schemes 2−4. The compounds that were initially chosen for synthesis contained the 3,4,5-trimethoxyphenyl (ring A) as the β-lactam N-1 and 4-methoxyphenyl as the β-lactam C-4 substituents, which are present in **2a**. β-Lactam synthesis was achieved with a Staudinger cycloaddition reaction between a ketene (generated from an acid chloride) and an imine under basic conditions.[33,37] The required imines **5a**−**f** were obtained by condensation reaction of the appropriately substituted benzaldehydes and anilines (Scheme 1). In the case of **5e**, the phenolic group present on the starting 3-hydroxy-4-methoxybenzaldehyde was first protected as the *tert*-butyldimethylchlorosilane (TBDMS) ether[38] which can be removed later under mild conditions with tetrabutylammonium flouride which is suitable for the stability of the β-lactam functional group.[39] Acid chlorides **6a**−**d** (Scheme 2) were prepared by reaction of the appropriately substituted acetic acids with thionyl chloride. For the preparation of the acid chloride **6c**, (3-hydroxylphenyl)acetic acid was first treated with benzyl bromide to

Scheme 1. Synthesis of Imines **5a**−**f**[a]

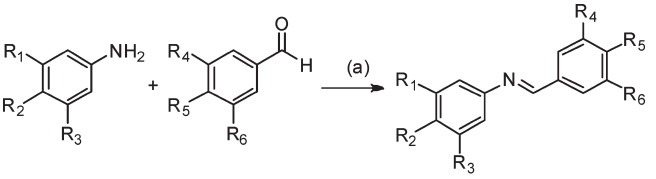

5a: $R_1=R_2=R_3=R_5=OCH_3$; $R_4=R_6=H$
5b: $R_1=R_2=R_3=R_4=R_6=H$; $R_5=OCH_3$
5c: $R_1=R_3=H$; $R_2=R_4=R_5=R_6=OCH_3$
5d: $R_1=R_2=R_3=H$; $R_4=R_5=R_6=OCH_3$
5e: $R_1=R_2=R_3=R_5=OCH_3$; $R_4=H$; $R_6=OSi(CH_3)_2C(CH_3)_3$
5f: $R_1=R_2=R_3=R_5=OCH_3$; $R_5=H$; $R_6=NO_2$

[a] Reagents and conditions: (a) EtOH, reflux, 3 h.

afford (3-benzyloxyphenyl)acetic acid.[40] The acid chloride **6d** is prepared from (4-aminophenyl)acetic acid on first reaction with benzyl chloroformate to afford the (4-benzyloxycarbonylaminophenyl)acetic acid,[41] which was then converted to the unstable acid chloride **6d** on reaction with thionyl chloride (Scheme 2, step a). The chlorination reactions were monitored by IR spectroscopy until acid chloride carbonyl absorption was observed (ν = 1790−1815 cm^{-1}).

The racemic β-lactam products **7**−**14** were obtained in low yields on treatment of the imines **5a**−**f** at reflux in dichloromethane with the appropriate acid chloride in the presence of triethylamine (Scheme 2, route I; one enantiomer only shown). β-Lactam compounds **15**−**17** were prepared using a modified procedure at room temperature, as they were not successfully obtained by the usual conditions of the Staudinger reaction (Scheme 2, route II). Failure to form β-lactams with 4-nitrophenylacetyl chloride under standard Staudinger conditions has previously been reported.[42] The stereochemistry of the β-lactam products obtained in Staudinger reactions depends on numerous factors, including the reaction conditions, the order of addition of the reagents, and the substituents present on both the imine and the acid chloride.[33,43] In the present reactions, the trans products were isolated exclusively in all cases, as evident from the ^{1}H NMR spectrum of compound **7** where the H-3 and H-4 were identified at δ 4.23 and δ 4.79, respectively, as a pair of coupled doublets, $J_{3,4}$ = 2.0 Hz.

The β-lactams **18**−**31** were obtained directly from the appropriate phenylacetic acid using an acid-activating agent in a one-step reaction (Scheme 2, route III), which was the reaction of choice for the majority of the products. Many acid-activating agents have been reported for this reaction, e.g., Mukaiyama's reagent (2-chloro-*N*-methylpyridinium iodide), ethyl chloroformate, trifluoroacetic anhydride, *p*-toluenesulfonyl chloride, and various phosphorus derived reagents including triphosgene, which was successfully used in the present study.[44]

Scheme 2. Synthesis of Azetidinones **7**−**31**: Routes I, II, and III[a]

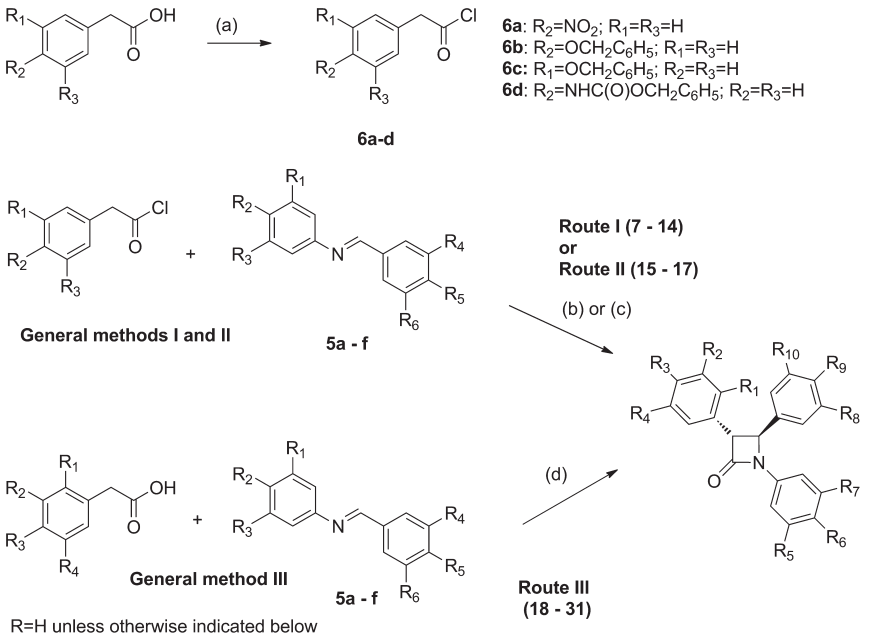

R=H unless otherwise indicated below

7: $R_3=R_8=R_9=R_{10}=OCH_3$
8: $R_2=R_5=R_6=R_7=R_9=OCH_3$
9: $R_3=R_5=R_6=R_7=R_9=OCH_3$
10: $R_2=R_3=R_5=R_6=R_7=R_9=OCH_3$
11: $R_3=Cl$; $R_5=R_6=R_7=R_9=OCH_3$
12: $R_3=OCH_2C_6H_5$; $R_5=R_6=R_7=R_9=OCH_3$
13: $R_3=F$; $R_5=R_6=R_7=R_9=OCH_3$; $R_8=OSi(CH_3)_2C(CH_3)_3$
14: $R_5=R_6=R_7=R_9=OCH_3$; $R_8=NO_2$
15: $R_3=NO_2$; $R_5=R_6=R_7=R_9=OCH_3$
16: $R_3=NHC(O)OCH_2C_6H_5$; $R_5=R_6=R_7=R_9=OCH_3$; $R_8=NO_2$
17: $R_3=F$; $R_5=R_6=R_7=R_9=OCH_3$; $R_8=NO_2$
18: $R_2=R_3=R_4=R_9=OCH_3$
19: $R_1=R_5=R_6=R_7=R_9=OCH_3$
20: $R_2=R_3=R_4=R_5=R_6=R_7=R_9=OCH_3$
21: $R_3=SCH_3$; $R_5=R_6=R_7=R_9=OCH_3$
22: $R_3=CH_3$; $R_5=R_6=R_7=R_9=OCH_3$
23: $R_3=Br$; $R_5=R_6=R_7=R_9=OCH_3$
24: $R_3=F$; $R_5=R_6=R_7=R_9=OCH_3$
25: $R_2=R_3=Cl$; $R_5=R_6=R_7=R_9=OCH_3$
26: $R_2=R_3=F$; $R_5=R_6=R_7=R_9=OCH_3$
27: $R_3=CF_3$; $R_5=R_6=R_7=R_9=OCH_3$
28: $R_2=OCH_2C_6H_5$; $R_5=R_6=R_7=R_9=OCH_3$
29: $R_3=OCH_2C_6H_5$; $R_5=R_6=R_7=R_9=OCH_3$; $R_8=OSi(CH_3)_2C(CH_3)_3$
30: $R_3=NHC(O)OCH_2C_6H_5$; $R_5=R_6=R_7=R_9=OCH_3$; $R_8=OSi(CH_3)_2C(CH_3)_3$
31: $R_3=OCH_2C_6H_5$; $R_5=R_6=R_7=R_9=OCH_3$; $R_8=NO_2$

[a] Reagents and conditions: (a) $SOCl_2$, $CHCl_3$, reflux, 3 h; (b) (route I) triethylamine, anhydrous CH_2Cl_2, reflux, 3 h; (c) (route II) triethylamine, anhydrous CH_2Cl_2, 20 °C, 18 h; (d) (route III) triphosgene, triethylamine, anhydrous CH_2Cl_2, reflux, 5 h; 20 °C, stirred 18 h.

Scheme 3. Synthesis of Azetidinones **32**−**34**: Route IV[a]

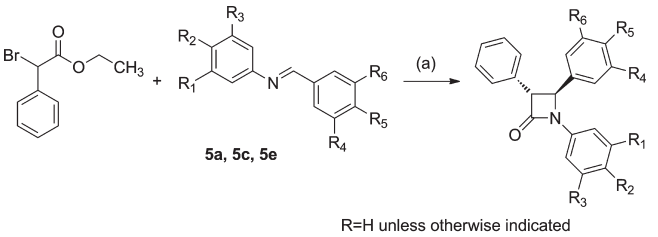

R=H unless otherwise indicated

32: $R_1=R_2=R_3=R_5=OCH_3$
33: $R_2=R_4=R_5=R_6=OCH_3$
34: $R_1=R_2=R_3=R_5=OCH_3$, $R_4=OSi(CH_3)_2C(CH_3)_3$

[a] Reagents and conditions: (a) zinc, trimethylchlorosilane, benzene, microwave.

Scheme 4. Synthesis of Azetidinones **35**−**38**: Route V[a]

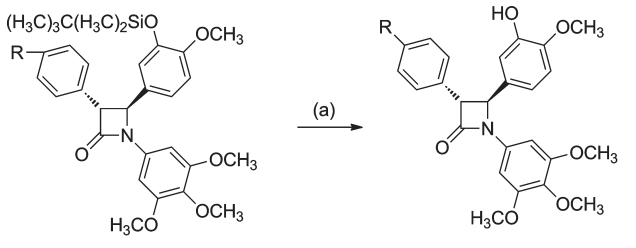

35: R=H
36: R=F
37: $R=OCH_2C_6H_5$
38: $R=NHC(O)OCH_2C_6H_5$

[a] Reagents and conditions: TBAF, THF, 0 °C, 15 min.

Trans stereochemistry was also observed for these products, e.g., for compound **18** where the H-3 and H-4 were identified at δ 4.20 and δ 4.89, respectively, as a pair of coupled doublets, $J_{3,4}$ = 2.5 Hz. With selected phenylacetic acid derivatives, this reaction was unsuccessful and the acids were converted to acid chlorides **6a**−**d**. β-Lactams were then obtained by the Staudinger route (route I) as described above.

In some cases, a Reformatsky reaction was used for the synthesis of the required β-lactam compounds (Scheme 3).[45,46] We have recently reported the application of the Reformatsky reaction to obtain 1,3-diarylazetidinones, which are unsubstituted at C-3 or contain methyl substituent(s) at C-3.[35] We now report the preparation of 1,3,4-triarylazetidinones using a Reformatsky reaction that has been adapted for microwave conditions. Previous investigations found TMCS to be superior for zinc activation[47] in Reformatsky reactions than either iodine or zinc washed with 10% nitric acid. We examined the use of zinc powder that was preactivated with trimethylchlorosilane in microwave conditions in the Reformatsky reactions, resulting in slightly increased yield of the desired β-lactam products **32**−**34** and a significant reduction in the reaction time from 8 h to 30 min (Scheme 3). In the present reactions,

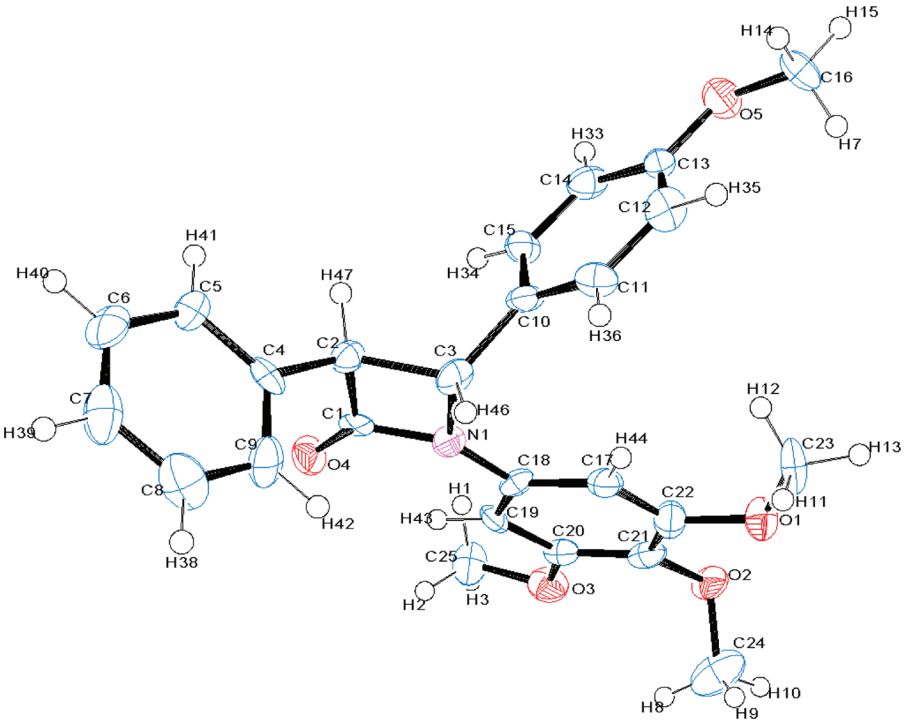

Figure 2. ORTEP representation of the X-ray crystal structure of azetidinone **32** with 50% thermal ellipsoids.

Scheme 5. Synthesis of Azetidinones **39**−**42**: Route VI[a]

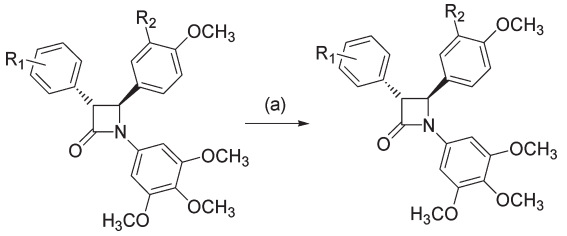

12: R_1=4-$OCH_2C_6H_5$; R_2=H
28: R_1=3-$OCH_2C_6H_5$; R_2=H
37: R_1=4-$OCH_2C_6H_5$; R_2=OH
31: R_1=4-$OCH_2C_6H_5$; R_2=NO_2

39: R_1=4-OH; R_2=H
40: R_1=3-OH; R_2=H
41: R_1=4-OH; R_2=OH
42: R_1=4-OH; R_2=NH_2

[a] Reagents and conditions: (a) H_2, Pd/C, EtOH/EtOAc (1:1).

the trans products were isolated exclusively in all cases, as evident from the ^{1}H NMR spectrum of compound **32** where the H-3 and H-4 were identified at δ 4.29 and δ 4.87 ppm, respectively, as a pair of coupled doublets, $J_{3,4}$ = 2.5 Hz. The trans configuration can be seen in the X-ray crystal structure of β-lactam **32** in Figure 2. The enantiomeric composition of compound **32** was clearly demonstrated on analysis by chiral HPLC (t_R of 11.93 and 12.53 min).

The phenolic products **35**, **36**, **37**, and **38** were obtained on treatment of the silyl ethers **13**, **29**, **30**, and **34**, respectively, with tetrabutylammonium fluoride at 0 °C (Scheme 4). Phenolic products **39**, **40**, **41**, and **42** were obtained by careful hydrogenolysis of the corresponding benzyl ethers **12**, **28**, **37**, and **31** respectively (Scheme 5). Reduction of the nitro group in compounds **15**, **14**, and **17** to the corresponding amines **43**, **44**, and **45**, respectively, was achieved by treatment with zinc dust and glacial acetic acid (Scheme 6). Treatment of the carbamate protected compounds **38** and **16** with hydrogen and palladium afforded the amines **46** and **47**, respectively (Scheme 7).

Scheme 6. Synthesis of Amino Substituted Azetidinones **43**−**45**: Route VII[a]

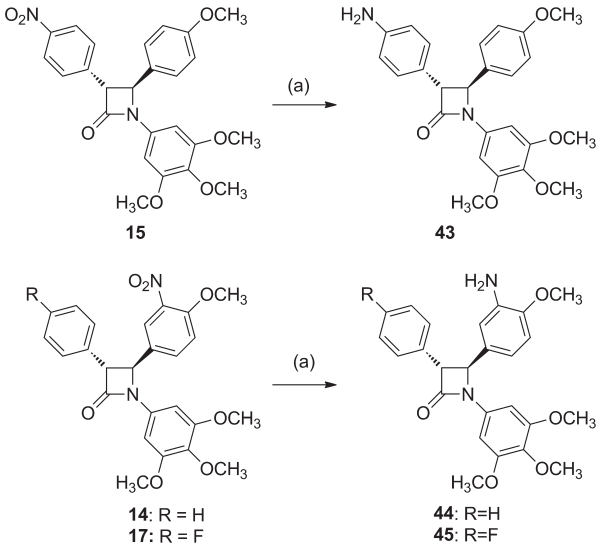

15 **43**

14: R = H
17: R = F

44: R=H
45: R=F

[a] Reagents and conditions: (a) Zn, CH_3CO_2H, 7 days.

To further investigate the contribution of the β-lactam carbonyl group to the activity of this compound class, a novel thione analogue **48** was prepared in good yield by reaction of the compound **32** with Lawesson's reagent (2,4-bis-(4-methoxyphenyl)-1,2,3,4-dithiaphosphetane 2,4-disulfide) (Scheme 8). The characteristic C=S absorption band was observed at ν = 1592.5 cm^{-1} for this product. A broad variety of β-lactams have been subjected to reductive ring-opening with metal hydrides to yield the corresponding γ-aminoalcohols.[48] To investigate the contribution of the intact β-lactam ring structure to the activity of this series of compounds, **35** was subjected to treatment with $LiAlH_4$ to afford the amino alcohol product **49** which was isolated by an acid−base extraction to

Scheme 7. Synthesis of Azetidinones **46** and **47**: Route VIII[a]

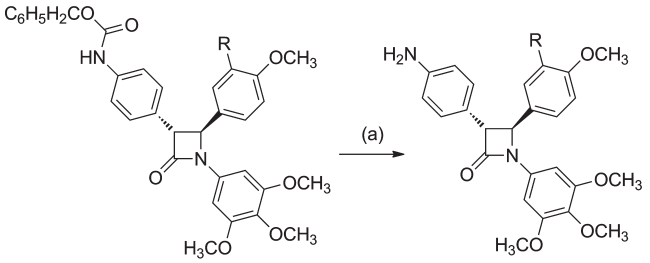

[a] Reagents and conditions: (a) H_2, Pd/C, EtOH/EtOAc (1:1).

Scheme 8. Synthesis of Azetidinthione **48**[a]

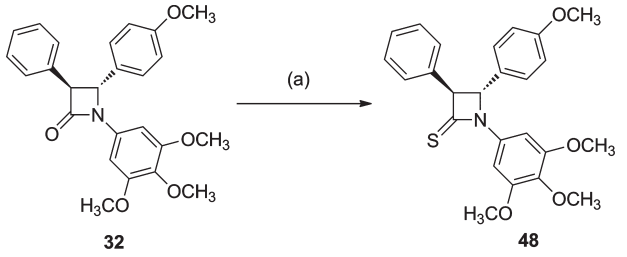

[a] Reagents and conditions: (a) Lawesson's reagent, toluene, reflux, 3 h.

Scheme 9. Azetidinone Reduction and Methanolysis[a]

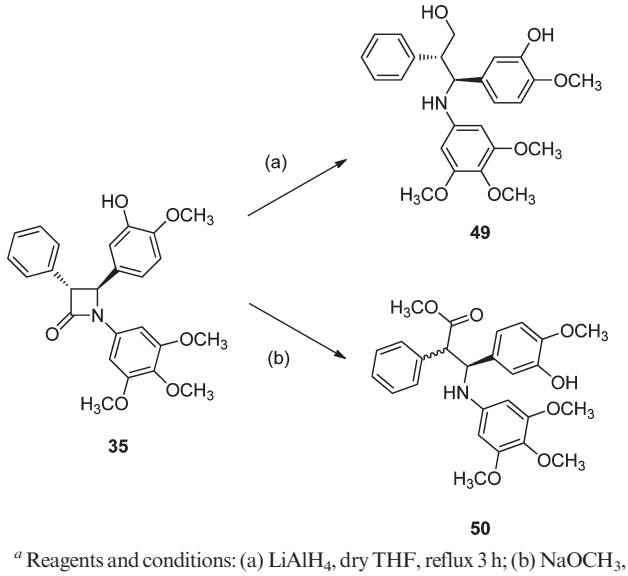

[a] Reagents and conditions: (a) $LiAlH_4$, dry THF, reflux 3 h; (b) $NaOCH_3$, MeOH, 20 °C, 8 days.

give the desired γ-amino alcohol (Scheme 9). Cleavage of the β-lactam N1−C2 bond usually takes place with nucleophilic reagents such as alkoxide ion.[49−52] The ease of hydrolysis is apparently a function of increasing size and number of substituents at the 3-position; with increased size and number hydrolysis becomes increasingly difficult.[53] A methoxide ring-opening reaction was carried out on **35** with 4 equivalents of sodium methoxide at room temperature over 8 days until reaction was complete on TLC. ^{1}H NMR analysis of the product **50** indicated formation of a diastereomeric product mixture (Scheme 9).[51,52] For methyl ester **50**, the presence of two amino signals at δ 5.75 ppm and δ 6.10 ppm is indicative of two isomers. There are also two signals for each of the α and β protons (formerly at positions 3 and 4 of the azetidinone ring) between δ 3 ppm and δ 5 ppm. In the ^{13}C NMR spectrum of **50**, there are two carbonyl signals at δ 171.55 ppm and δ 172.70 ppm.

The structures of the various β-lactams synthesized are illustrated in Tables 1, 2, and 3, together with their routes of synthesis. Table 1 lists the initial β-lactams with the methoxy functionalities at different positions of the β-lactam scaffold. The comprehensive series of β-lactams prepared with structural modification of the aryl ring at the C-3 position of the β-lactam heterocycle are listed in Table 2. Finally, Table 3 shows further phenolic and amino modifications to the initial series of compounds with the aim of improving activity. Compounds **32** and **35** were selected for chemical stability analysis and further development based on the analysis of their drug-like (Lipinski) properties together with predictions of permeability, metabolic stability, Pgp substrate status, blood−brain barrier partition, plasma protein binding, and human intestinal absorption properties. The stability of the target compounds **32** and **35** was evaluated in phosphate buffer at pH 4, 7.4, and 9, and the half-life was determined to be greater than 24 h for each compound at these pH values.

Antiproliferative Activity

These analogues were first evaluated for their antiproliferative activity in the MCF-7 (ER-positive) human breast cancer cell line, and the most potent compounds were then screened against the MDA-MB-231 cell line (ER-negative). The activities of the azetidin-2-ones are presented in Tables 4 and 5. In addition, compounds **32** and **35** were evaluated in the NCI-60 cell line screen (Table 9, Supporting Information). Initially, the azetidin-2-ones prepared containing a 4-methoxy substituent on the C-4 phenyl ring were examined (compounds **7**−**12**, **14**, **15**, **17**−**27**, **32**). From these early lead compounds, a more extensive series of active derivatives were synthesized containing the 3-hydroxy-4-methoxy and 3-amino-4-methoxy substitution pattern on the C-4 phenyl ring, (compounds **35**, **36**, **39**−**47**). This latter series of compounds was designed to contain structural features similar to those of **1**, **2a**, and the CA-4 amino analogue (**3a**).

The positions of the 3,4,5-trimethoxyphenyl and 4-methoxyphenyl ring substitution were initially examined at different locations on the azetidinone ring (compounds **7**, **18**, **32**, and **33**) (Table 4). **2a** was used as the positive control. The optimal positioning was found to be in compound **32** (IC_{50}(MCF-7) = 34 nM), where the 3,4,5-trimethoxyphenyl ring is located at the N-1 position and the 4-methoxyphenyl ring is at the C-4 position, as previously observed by Sun et al. for other β-lactam compounds.[34] Any other arrangement of these two rings was significantly less active than **32** by a factor of over 1000. The effect of the introduction of substituents onto the C3-aryl ring of compound **32** was next investigated. In the 3-aryl substituted series (compounds **7**−**31**), larger substituents such as 3,4,5-trimethoxyphenyl (**20**), 4-trifluoromethylphenyl (**27**), and 4-benzyloxyphenyl (**12**) were not tolerated and led to a significant decrease in activity against MCF-7 cells. The most active analogues in this series were found to be those with small, polar substituents including examples **24** (4-fluorophenyl), **39** (4-hydroxyphenyl), **40** (3-hydroxyphenyl), and **43** (4-aminophenyl) with IC_{50} values in MCF-7 cells of 42, 59, 68, and 50 nM, respectively.

The activity of the series was further optimized by modification of the C-4 aryl substituent of the azetidinone ring to

Table 1. Azetidinones with Methoxy Substitution at N-1, C-3, and C-4 Aryl Rings

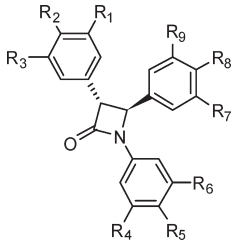

compd	R_1	R_2	R_3	R_4	R_5	R_6	R_7	R_8	R_9	route for synthesis
7	H	OCH_3	H	H	H	H	OCH_3	OCH_3	OCH_3	I
18	OCH_3	OCH_3	OCH_3	H	H	H	H	OCH_3	H	III
32	H	H	H	OCH_3	OCH_3	OCH_3	H	OCH_3	H	IV
33	H	H	H	H	OCH_3	H	OCH_3	OCH_3	OCH_3	IV

Table 2. Azetidinones with C-3 Aryl Substitution

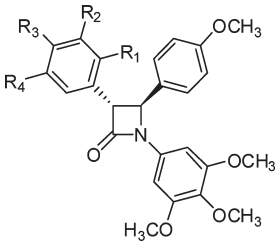

compd	R_1	R_2	R_3	R_4	route for synthesis
8	H	OCH_3	H	H	I
9	H	H	OCH_3	H	I
10	H	OCH_3	OCH_3	H	I
11	H	H	Cl	H	I
12	H	H	$OCH_2C_6H_5$	H	I
15	H	H	NO_2	H	II
19	OCH_3	H	H	H	III
20	H	OCH_3	OCH_3	OCH_3	III
21	H	H	SCH_3	H	III
22	H	H	CH_3	H	III
23	H	H	Br	H	III
24	H	H	F	H	III
25	H	Cl	Cl	H	III
26	H	F	F	H	III
27	H	H	CF_3	H	III
28	H	$OCH_2C_6H_5$	H	H	III
32	H	H	H	H	IV
39	H	H	OH	H	II, VI
40	H	OH	H	H	III, VI
43	H	H	NH_2	H	II, VII

Table 3. Azetidinones with Hydroxyl and Amine-Type Substituents on C-3 and C-4 Aryl Rings and Related Compounds

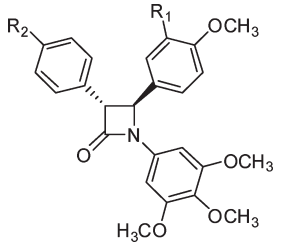

compd	R_1	R_2	route for synthesis
13	$OSi(CH_3)_2C(CH_3)_3$	F	I
14	NO_2	H	I
16	NO_2	$NHC(O)OCH_2C_6H_5$	II
17	NO_2	F	II
29	$OSi(CH_3)_2C(CH_3)_3$	$OCH_2C_6H_5$	III
30	$OSi(CH_3)_2C(CH_3)_3$	$NHC(O)OCH_2C_6H_5$	III
31	NO_2	$OCH_2C_6H_5$	III
34	$OSi(CH_3)_2C(CH_3)_3$	H	IV
35	OH	H	IV, V
36	OH	F	I, V
37	OH	$OCH_2C_6H_5$	III, V
38	OH	$NHC(O)OCH_2C_6H_5$	III, V
41	OH	OH	III, VI, VI
42	NH_2	OH	III, VI
44	NH_2	H	I, VII
45	NH_2	F	II, VII
46	OH	NH_2	III, V, VIII
47	NH_2	NH_2	II, VIII

include either a hydroxy or an amino group as in compounds **35**−**38** and **41**−**47** (Schemes 4−7, Table 4). Analogues of the three most active compounds from Table 2 were synthesized with both 4-(3-hydroxy-4-methoxyphenyl) and 4-(3-amino-4-methoxyphenyl) substitution (Table 3). With one exception, the 3-hydroxy-4-methoxy substituted analogues were over 10-fold more active than their corresponding 3-amino-4-methoxy derivatives (compare **41** to **42**, for example, with IC_{50} values of 0.8 and 39.5 nM, respectively, in MCF-7 cells). The exception was the fluorinated analogues, in which the introduction of an amino substituent to the C-4 phenyl ring of **24** resulted in a slight increase in potency (compound **45**) when compared to the hydroxyl analogue **36**, and both were less active than compound **24** (IC_{50} values of 55, 66, and 42 nM, respectively, in MCF-7 cells). The activity of nitro-substituted compound **17** is included for comparison (IC_{50} of 1.4 μM), indicating the critical importance of a polar H-bonding substituent on the C-3 phenyl ring. The phenolic hydroxyl group is the optimal substituent at the 3-position of the 4-phenyl ring. The most potent compound in the series, **41**, displayed subnanomolar antiproliferative activity in the MCF-7 cell line with an IC_{50} of 0.8 nM. Figure 3 shows a dose-response result for the antiproliferative effect of β-lactam compounds **32** and **41** in MCF-7 cells. Compound **46**, containing a 3-(4-aminophenyl) substituent, also showed greater activity than the lead compound **32**, with an IC_{50} of 4 nM in MCF-7 cell line.

The replacement of the β-lactam carbonyl group with the thione in compound **48** resulted in a reduction in the observed

Table 4. Antiproliferative Effects of Azetidinones in MCF-7 Human Breast Cancer Cells

compd	antiproliferative activity[a] MCF-7 cells IC_{50} (μM)	compd	antiproliferative activity[a] MCF-7 cells IC_{50} (μM)
7	37.75 ± 23.35	**27**	1.6577 ± 0.4283
8	0.3263 ± 0.1565	**32**	0.0344 ± 0.0198
9	0.1820 ± 0.0262	**33**	43.12 ± 16.47
10	0.2228 ± 0.1585	**35**	0.0096 ± 0.0026
11	0.3052 ± 0.1380	**36**	0.0657 ± 0.0056
12	7.9857 ± 1.8590	**39**	0.0591 ± 0.0198
14	0.4663 ± 0.0361	**40**	0.0689 ± 0.0592
15	0.4856 ± 0.2815	**41**	0.0008 ± 0.0004
17	1.3642 ± 0.74	**42**	0.0395 ± 0.0216
18	43.13 ± 20.44	**43**	0.0508 ± 0.0194
19	0.6995 ± 0.1874	**44**	0.0653 ± 0.0111
20	7.1193 ± 3.9135	**45**	0.0553 ± 0.0087
21	0.4480 ± 0.2304	**46**	0.0045 ± 0.0032
22	0.3152 ± 0.0714	**47**	0.0309 ± 0.0357
23	0.4196 ± 0.0817	**48**	0.72 ± 0.47
24	0.0423 ± 0.0420	**49**	24.5600 ± 2.6196
25	3.3607 ± 1.0377	**50**	> 100
26	0.3139 ± 0.1792	**2a**[b]	0.0052 ± 0.002

[a] IC_{50} values are half maximal inhibitory concentrations required to block the growth stimulation of MCF-7 or MDA-MB-231 cells. Values represent the mean ± SEM (error values × 10^{-6}) for three experiments performed in triplicate. [b] The IC_{50} value obtained for **2a** in this assay is 0.0052 μM for MCF-7 and is in good agreement with the reported values for **2a** using the MTT assay on human MCF-7 breast cancer cell lines, (see refs 7, 73, and 74).

Table 5. Antiproliferative Effects of Selected β-Lactam Compounds in MDA-MB-231 Human Breast Cancer Cells

compd	antiproliferative activity[a] MDA-MB-231 cells IC_{50} (μM)	compd	antiproliferative activity[a] MDA-MB-231 cells IC_{50} (μM)
24	0.2284 ± 0.1755	**41**	0.1764 ± 0.1578
32	0.0782 ± 0.0348	**42**	1.6839 ± 1.9756
35	0.0288 ± 0.0199	**43**	0.2245 ± 0.1778
36	0.1072 ± 0.0558	**44**	0.4288 ± 0.0670
39	0.1577 ± 0.0352	**45**	0.0808 ± 0.0738
		2a[b]	0.043

[a] IC_{50} values are half maximal inhibitory concentrations required to block the growth stimulation of MCF-7 or MDA-MB-231 cells. Values represent the mean ± SEM (error values × 10^{-6}) for three experiments performed in triplicate. [b] The IC_{50} values obtained for **2a** in this assay are 0.043 μM for MDA-MB-231 and is in good agreement with the reported values for **2a** using the MTT assay on MDA-MB-231 breast cancer cell lines (see refs 7, 73, and 74).

antiproliferative activity (IC_{50} = 0.72 μM for MCF-7 cells and IC_{50} = 0.89 μM for MDA-MB 231 breast cancer cells). The β-lactam ring is strained and can undergo a number of ring-opening reactions. In the present work, two ring-opened products were also synthesized and evaluated for antiproliferative activity to assess the lactam scaffold dependence of biological activity. Alcohol **49** is the result of treatment of **35** with lithium aluminum hydride, while ester **50** is the product from the nucleophilic ring-opening reaction of **35** with sodium methoxide. These compounds are more flexible than the rigid β-lactam parent compound **35**. They show over 2000-fold decrease in antiproliferative activity, indicating the critical importance of the rigid β-lactam scaffold and the relative orientations of the two methoxy-containing aromatic rings for preservation of antiproliferative activity. The importance of the relative orientations of the two aromatic rings has also been noted previously for CA-4.[22]

The more potent compounds in the MCF-7 cell line were next examined in an ER-negative MDA-MB-231 cell line, and

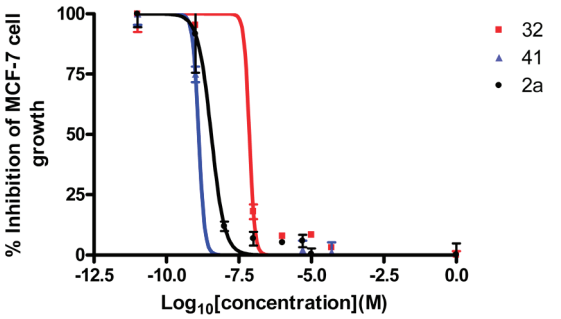

Figure 3. Antiproliferative effect of β-lactam compounds **32** and **41** alongside **2a** in MCF-7 human breast cancer cells. MCF-7 cells were seeded at a density of 2.5 × 10^4 cells per well in 96-well plates. The plates were left for 24 h to allow the cells to adhere to the surface of the wells. A range of concentrations (0.01 nM to 50 μM) of the compound were added in triplicate and the cells left for another 72 h. Control wells contained the equivalent volume of the vehicle ethanol (1% v/v). An MTT assay was performed to determine the level of antiproliferation. The values represent the mean ± SEM (error values) for three experiments performed in triplicate.

the results are displayed in Table 5. Compound **35** was found to be the most effective of the series with IC_{50} value of 28 nM; compounds **32** and **45** are also seen to be effective, with IC_{50} values of 78 and 80 nM, respectively. Compound **41** was also evaluated in the leukemia cell lines HL-60 and K562 and was found to be extremely potent with IC_{50} values of 0.34 and 0.89 nM, respectively, which compared favorably with the control **2a** [IC_{50} values of 1.99 nM (HL-60) and 3.68 nM (K562)].

On the basis of their potency, compounds **9** and **35** were evaluated in the National Cancer Institute (NCI)/Division of Cancer Treatment and Diagnosis (DCTD)/Developmental Therapeutics Program (DTP),[54] in which the activity of each compound was determined using approximately 60 different cancer cell lines of diverse tumor origins. These studies were performed at the NCI as part of their drug-screening program. Compounds **9** and **35** were tested for inhibition of growth (GI_{50}) and for cytotoxicity (LC_{50}) in the NCI panel of 56 cell lines and showed broad-spectrum antiproliferative activity against tumor cell lines derived from leukemia, breast cancer, non-small-cell lung cancer, colon cancer, CNS cancer, melanoma, ovarian cancer, renal cancer, and prostate cancer (see Table 9, Supporting Information). β-Lactam **9** showed submicromolar GI_{50} values in all but five cell lines (the GI_{50} value is the concentration of drug required for 50% inhibition of cellular growth). The mean GI_{50} value for compound **9** across all cell lines is 0.21 μM [log GI_{50} = −6.67 M]. For compound **35**, the GI_{50} values obtained were below 10 nM for 38 of the cell lines investigated, including breast cancers MCF-7, MDA-MB-231, and the adriamycin resistant NCI/ADR-RES cell line, with the mean GI_{50} value across all cell lines being 23.99 nM, [log GI_{50} = −7.62 M]. LC_{50} values are a measure of the cytotoxicity of these compounds and were greater than 100 μM for compound **9** in all but 3 cell lines and greater than 100 μM for compound **35** in all but 10 cell lines (Table 9, Supporting Information). These results confirm the requirement for the 3-hydroxy-4-methoxy substitution pattern on ring B for optimum antiproliferative activity in these analogues.

COMPARE Analysis of β-Lactams 9 and 35

Matrix COMPARE analysis[55,56] (measuring the correlation between two compounds with respect to their differential antiproliferative activity) demonstrated good correlation between **35** and **2a** (r = 0.62) and with other tubulin binding drugs

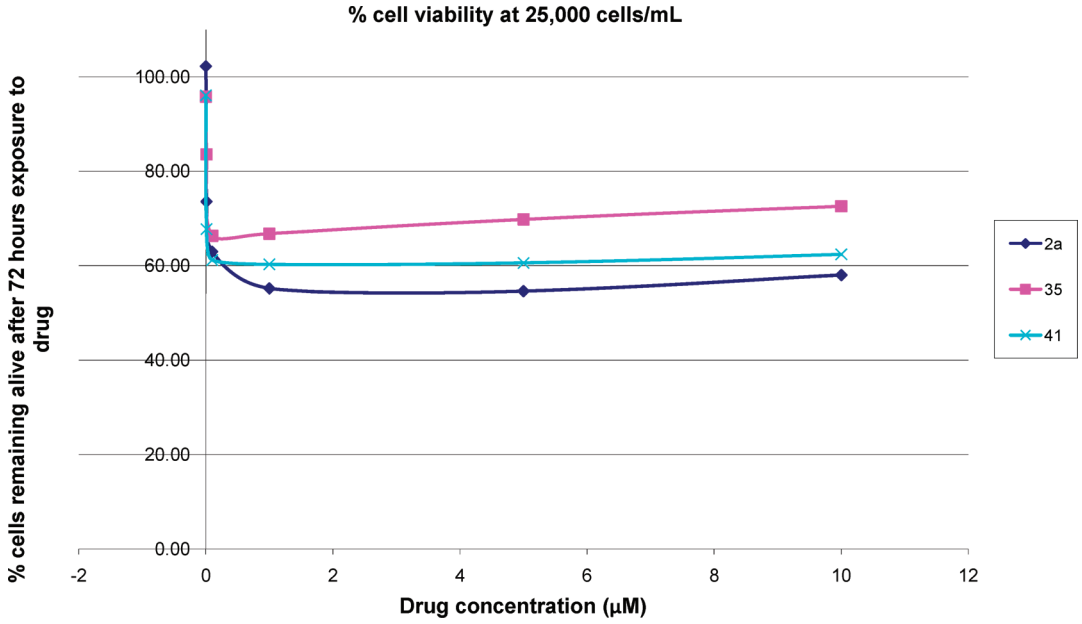

Figure 4. Dose-response curve for β-lactams **35**, **41**, and **2a** in murine mammary epithelial cells at 25 000 cells/mL. Mouse mammary epithelial cells were harvested from mid- to late-pregnant CD-1 mice and cultured. The isolated mammary epithelial cells were seeded at two concentrations. After 24 h, they were treated with 2 μL volumes of test compound which had been preprepared as stock solutions in ethanol to furnish the concentration range of study, 1 nM to 100 μM, and reincubated for a further 72 h. Control wells contained the equivalent volume of the vehicle ethanol (1% v/v). The cytotoxicity was assessed using alamarBlue dye.

vincristine, vinblastine, paclitaxel, maytansine, and rhizoxin (Table 10, Supporting Information). However, this algorithm does not distinguish between different tubulin-based mechanisms of action.[57] In vitro tubulin-binding studies confirmed that **35** is acting as a tubulin-binding agent. The antiproliferative activity observed for these compounds indicated that there is a significant therapeutic window between the concentration required for cancer cell growth inhibition and the concentration that is toxic to cells.

Evaluation of Toxicity in Normal Murine Mammary Epithelial Cells

Two of the most potent β-lactam compounds from antiproliferative studies in the MCF-7 cell line, **35** and **41**, were evaluated further for cytoxicity in murine mammary epithelial cells. **2a** was used as the positive control. Mouse mammary epithelial cells were harvested from mid- to late-pregnant CD-1 mice and cultured as described previously.[58,59] Two different cell concentrations were used in the toxicity assay: 25 000 and 50 000 cells/mL. The results are presented in Figure 4 and in the Supporting Information (Figures 10−12). The IC_{50} value is greater than 10 mM for the three compounds evaluated. This is further evidence that these β-lactam compounds are minimally toxic to nonproliferating cells.

Tubulin Binding Studies

The effects of representative β-lactam CA-4 analogues on the assembly of purified bovine tubulin were evaluated. Compounds **32**, **35**, and **41** which demonstrated potent antiproliferative effects in vitro were assessed. The ability of **2a** to effectively inhibit the assembly of tubulin was assessed as a positive control. Tubulin polymerization was determined by measuring the increase in absorbance over time at 340 nm. The V_{max} value offers the most sensitive indicator of tubulin/ligand interactions, and hence, V_{max} values were calculated for each test compound. Fold changes in V_{max} values for

Table 6. Inhibition of Tubulin Polymerization for Compounds **32**, **35**, **41**, and **2a**[a]

compd	fold-reduction in V_{max} at 10 μM
2a	6.0 ± 1.4
32	6.1 ± 0.9
35	8.3 ± 2.6
41	11.76 ± 3.85

[a] Effects of **2a**, **32**, **35** and **41** on in vitro tubulin polymerization. Purified bovine tubulin and GTP were mixed in a 96-well plate. The reaction was started by warming the solution from 4 to 37 °C. **2a** (10 μM) was used as a reference, while ethanol (1% v/v) was used as a vehicle control. The effect on tubulin assembly was monitored in a Spectramax 340PC spectrophotometer at 340 nm at 30 s intervals for 60 min at 37 °C. Fold inhibition of tubulin polymerization was calculated using the V_{max} value for each reaction. The results represent the mean ± standard error of the mean for three separate experiments.

polymerization curves of each test compound with reference to ethanol control were calculated and are detailed in Table 6. As anticipated, the active β-lactam CA-4 analogues **32**, **35**, and **41** inhibited the polymerization of tubulin (Table 9, Supporting Information). In more detail, the active β-lactams when evaluated at 10 μM, reduced the V_{max} value for the rate of tubulin polymerization from 6-fold for **2a** to 11.7-fold for compound **41** and to 8.3-fold for compound **35**, while compound **32** showed a 6-fold reduction in the value for V_{max}. This value is comparable if not superior to the rate of inhibition of tubulin assembly (6-fold) observed with **2a**. An IC_{50} value of 3.65 μM was calculated for compound **41** for the reduction in V_{max}, while an IC_{50} value of 4.89 μM was obtained for the effect in overall polymer mass (calculated from area under the polymerization curve). Inhibition of tubulin polymerization for compound **41** is illustrated in Figure 5. The tubulin binding studies clearly demonstrated that tubulin is the target of these new compounds; however, the specific binding site on tubulin was not investigated, for example, by use of a radiolabeled colchicine displacement assay. On the basis of the very close 3D structural similarity between the ligands **1**, **2a**, and the

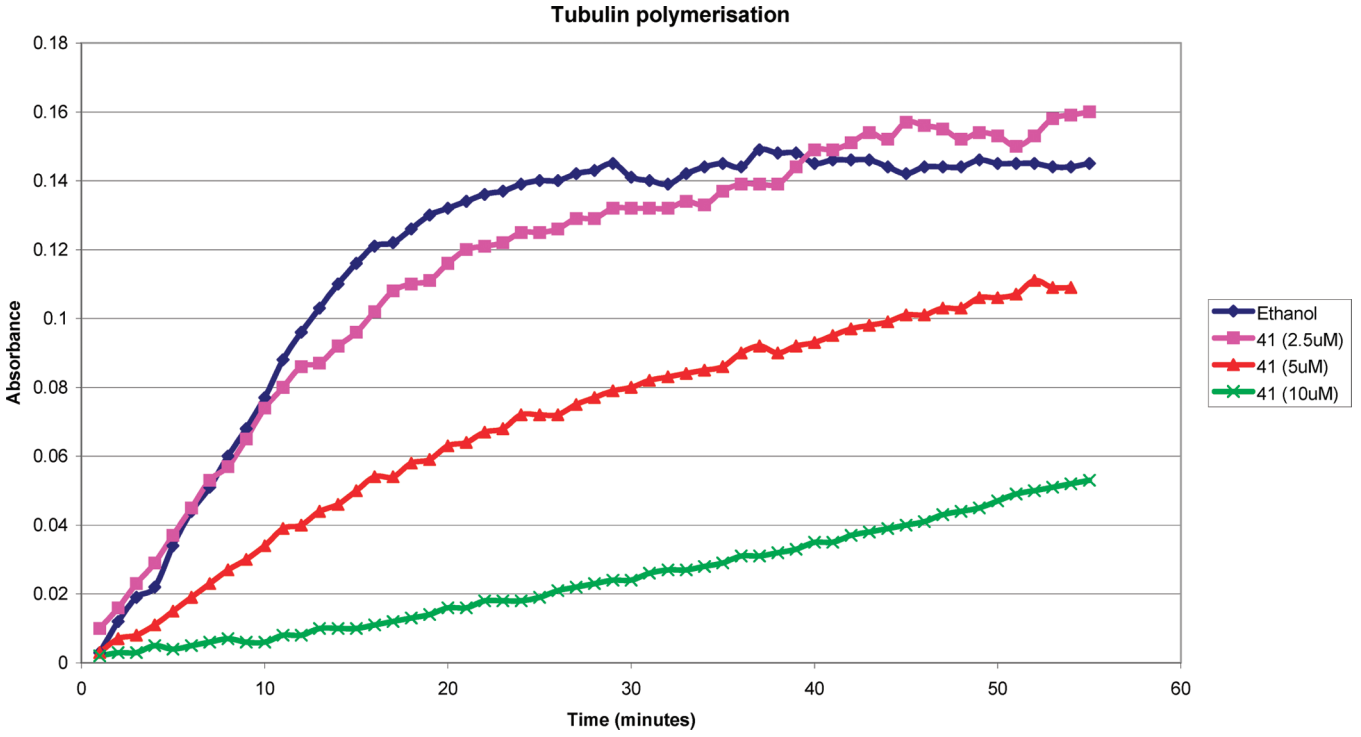

Figure 5. Effects of compound **41** on in vitro tubulin polymerization. Purified bovine tubulin and GTP were mixed in a 96-well plate. The reaction was started by warming the solution from 4 to 37 °C. **2a** (10 μM) was used as a reference, while ethanol (1%v/v) was used as a vehicle control. The effect on tubulin assembly was monitored in a Spectramax 340PC spectrophotometer at 340 nm at 30 s intervals for 60 min at 37 °C. Fold inhibition of tubulin polymerization was calculated using the V_{max} value for each reaction. The results represent the mean ± standard error of the mean for three separate experiments.

β-lactam analogues reported in this study (Figures 6B and 7D), we propose that the binding site for these compounds is most likely to be the colchicine site, since it has been demonstrated that **2a** and many reported examples of the structurally related conformationally constrained **2a** analogues bind at the colchicine site.[27,60,61]

Structural and Molecular Modeling Studies of Selected Azetidinones

The molecular structure of a representative example of the active series, compound **32**, was determined by single-crystal X-ray crystallography. The ORTEP diagram is presented in Figure 2, where the trans configuration at positions 3 and 4 of the β-lactam ring is clearly seen (note that in the X-ray numbering scheme in Figure 2, the carbon at the 3-position of the β-lactam ring is denoted as C2 and the carbon the 4-position of the β-lactam ring is denoted as C3). The structure revealed a conformation for the azetidinone **32** in which the two aromatic rings located at N-1 and C-4 are not coplanar. The rigid azetidinone ring provides a scaffold that can accommodate the steric and geometric requirements of the aromatic pharmacophores for tubulin binding. Ligands that bind at the colchicine-binding site of tubulin have the common feature of a trimethoxy aromatic ring, noted for such ligands as **1**, **2a**, and **4**.

The azetidinone **32** is structurally similar to **1** and **2a**, with the common structural features of a trimethoxyphenyl ring and a second aromatic ring substituted with methoxy groups in a noncoplanar diaryl system, with the observed tortional angle for ring A−ring B of 46.9° compared to 55° and 53° for the corresponding rings in **2a**[62] and **1**,[63] respectively. These structural similarities support the observed antiproliferative and tubulin polymerization inhibitory activity for these compounds as tubulin-targeting agents. The X-ray crystal structures of **2a**[62] and **2b**[22] suggest that the conformation of this stilbene is not planar. These crystal structures reveal that the planes of the two phenyl rings are inclined to each other, suggesting a low-energy conformation that may be the one involved in binding at the tubulin receptor site.[22]

To rationalize the potential binding modes of these β-lactam compounds in tubulin, docking studies were carried out with two of the most potent compounds in the 3-aryl β-lactam series, **32** and **41**. By use of the reported X-ray structure of tubulin cocrystallized with a colchicine derivative, *N*-deacetyl-*N*-(2-mercaptoacetyl)colchicine (DAMA-colchicine, PDB entry 1SA0), possible binding orientations for **32** and **41** were probed with the docking program FRED, version 2.2.3 (Openeye Scientific Software).[64] Because of the structural similarity between the β-lactams and colchicine site ligands such as **2a**, it was proposed that **32** and **41** bind to tubulin at the colchicine-binding site. The colchicine-binding site in tubulin is mainly buried in the β-subunit while maintaining few interactions with the α-subunit; there is one such site on each tubulin heterodimer. The H7 and H8 α-helices, the T7 loop, and the S8 and S9 β-strands contribute to the binding site and interact with the ligand. Two important residues for binding of colchicine-type ligands to tubulin have been identified as Val β318 and Cys β241.[63] Val β318 tubulin variants have reduced sensitivity to **1**, and colchicine substituted with more reactive groups instead of the methoxys can be cross-linked with Cys β241.[63]

Molecular modeling studies were carried out with the β-lactam compounds synthesized and evaluated to determine if these interactions were predicted to be present. Figure 6A illustrates β-lactam **32** docked in the colchicine-binding site of tubulin, while Figure 7A and Figure 7B show similar graphics with β-lactam **41** docked. β-Lactam **41** was the most active compound in antiproliferative assays and also in the tubulin polymerization

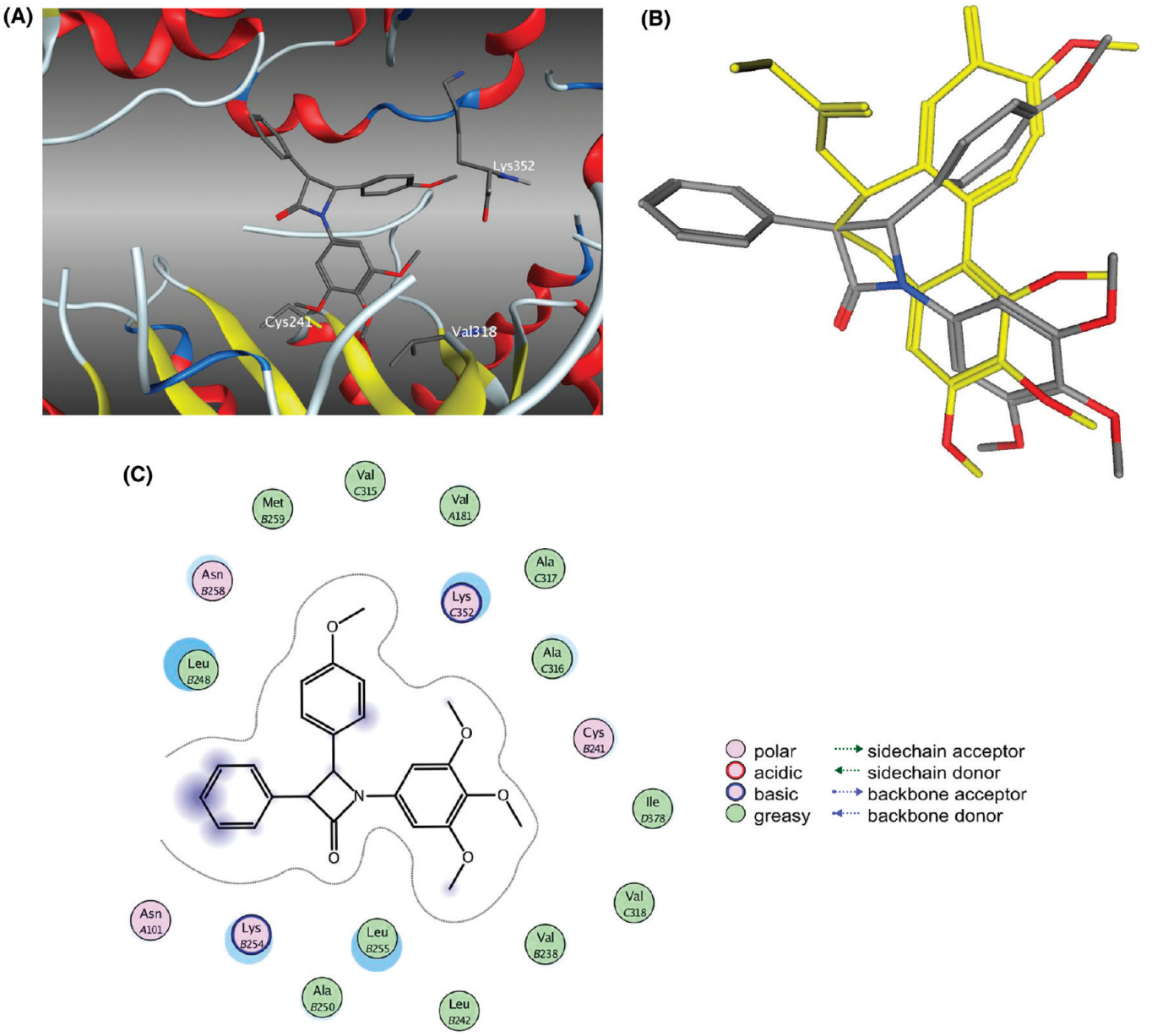

Figure 6. (A) Docked pose of β-lactam **32** in the colchicine binding site of tubulin (PDB entry 1SA0). Significant binding residues Cys 241 and Val 318 are indicated. Hydrogens are not shown for clarity. Coloring is by atom: gray (carbon); red (oxygen); blue (nitrogen); yellow (sulfur). Residue numbers are those used by Ravelli et al.[63] (B) Docked pose of **32** (colored by atom) overlaid with *N*-deacetyl-*N*-(2-mercaptoacetyl)-colchicine (DAMA-colchicine) (yellow) in the tubulin binding site (PDB entry 1SA0). Residues are not shown for clarity. (C) 2D representation of the binding of β-lactam **32** in the colchicine-binding site of tubulin: 2-D rendering of ligand−protein interactions using LigX module of MOE used to create docked structures of **32** in the colchicine-binding site of tubulin.

inhibition assay. The two important residues for binding in the colchicine-binding site of tubulin are identified as Val β318 and Cys β241. Figures 6A, 7A, and 7B show that the trimethoxy rings of both **32** and **41** are well positioned in proximity to the Cys241 residue (residue numbers are those used by Ravelli et al[63]), and the compounds adopt an orientation very similar to that of the trimethoxy ring of DAMA-colchicine in the cocrystallized structure. In addition, for compound **41**, Thr 179 is seen to establish a strong H-bond to the 3-OH substituent of ring B (Figure 7A, Figure 7B). This residue has previously been identified as interacting with a number of colchicine site ligands.[32,65,66] This interaction may also explain the binding of the related compound in the series with an OH substituent in similar position (e.g., compounds **35**, **36**, **46**) and also the related analogues with NH_2 substituent at C-3 of the aryl B-Ring. Activity is optimized by additional substituents on the C-3 aryl such as 4-F, 4-NH_2, 4-OH, 3-OH (compounds **24**, **39**, **40**, **43**) which preserve the key interactions with active residues for ring A and ring B. The H-bonding interaction between the 4-hydroxyaryl group at the 3-position of β-lactam **41** and the Lys 254 residue (Figure 7A, 7B), in addition to hydrophobic contacts with the 3-phenyl ring (not shown for clarity), could contribute to the observed higher antiproliferative activity observed for this analogue. The hydrophobic interactions are illustrated in Figure 7C and include interactions of the 3-phenyl ring with Leu248, Ala250, and Leu255. Activity is significantly reduced for β-lactam analogues of **32** that have multiple methoxy substitutions on the C-3 aryl ring as in compound **20** or increased steric hindrance with the benzyloxy ether (compound **28**).

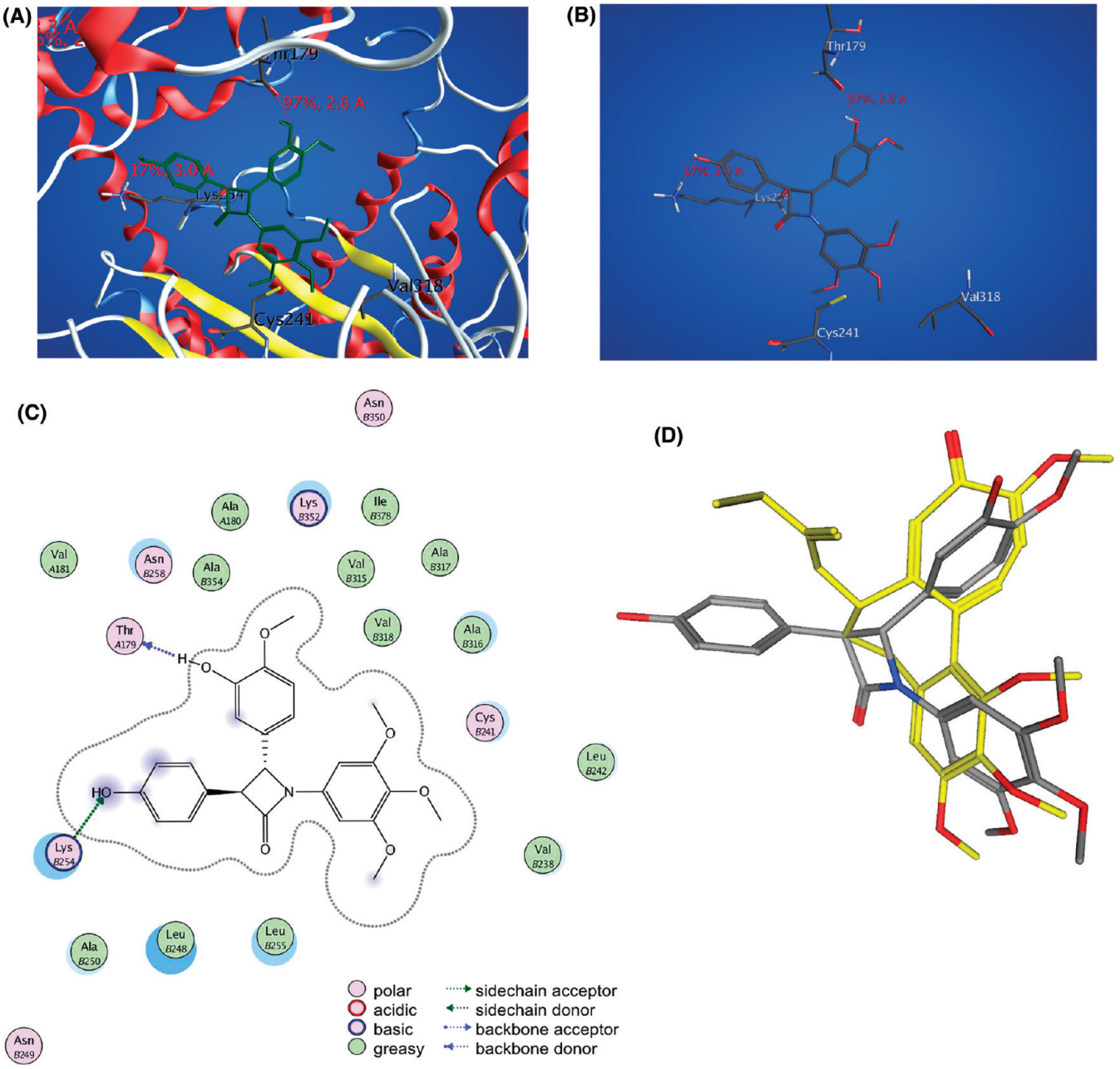

Figure 7. (A) Proposed binding and docked pose of β-lactam **41** (green) in colchicine binding site of tubulin (PDB entry 1SA0). Hydrogens are not shown for clarity. Significant binding residues Thr179, Cys241, Val318, and Lys254 are indicated. Residue numbers are those used by Ravelli et al.[63] (B) Docked pose of β-lactam **41** in colchicine binding site of tubulin (PDB entry 1SA0) with isolated important residues. Hydrogens are not shown for clarity. Significant binding residues Cys241, Val318, and Lys254 are indicated. Coloring is by atom: gray (carbon); red (oxygen); blue (nitrogen); yellow (sulfur). Residue numbers are those used by Ravelli et al.[63] (C) 2D representation of the binding of β-lactam **41** in the colchicine-binding site of tubulin: 2-D rendering of ligand−protein interactions using LigX module of MOE used to create docked structures of **41** in the colchicine-binding site of tubulin. (D) Docked pose of **41** (colored by atom) overlaid with *N*-deacetyl-*N*-(2-mercaptoacetyl)colchicine (DAMA-colchicine) (yellow) in the tubulin binding site (PDB entry 1SA0). Residues are not shown for clarity.

Several other hydrophobic contacts are predicted to stabilize the binding of **32** and **41** to tubulin. Figures 6C and 7C depict the predicted binding interactions of docked β-lactams **32** and **41** in 2D format.[67] From these results it can be seen that the important interactions discussed above are predicted to be present for these compounds. The docked pose of **32** (colored by atom) overlaid with colchicine (yellow) in the tubulin binding site is illustrated in Figure 6B. It can be seen that the methoxy substituent of ring B is in proximity in the binding site to the corresponding methoxy group on ring C of colchicine. A similar binding orientation is observed for colchicine and **41** (Figure 7D). These binding parallels may rationalize the potency observed for **32** and **41** in their inhibition of tubulin polymerization.

Conclusion

We have synthesized a comprehensive series of β-lactam compounds that show potent antiproliferative activity in a range of tumor cell lines, notably in human breast cancer MCF-7 and MDA-MB-231 cell lines. The most potent compound in the series **41** displayed subnanomolar activity in the MCF-7 cell line with an IC_{50} of 0.8 nM. Compound **46**

containing a 3-(4-aminophenyl) substituent also showed greater activity than the lead compound **32**, with an IC_{50} of 4 nM in MCF-7 cell line, with the 3-phenylsubstituted β-lactam **32** having an IC_{50} of 34 nM. The compounds did not cause significant cytotoxicity in normal murine breast epithelial cells. Compounds **32**, **35**, and **41** were shown to inhibit the polymerization of tubulin with improved efficacy when compared with **2a**.

X-ray crystal structure of **32** revealed that the compound provides a scaffold structure with a similar spatial arrangement between the two phenyl rings as observed in cis configuration of **2a**. Preliminary modeling studies indicate a possible binding mode for these potent inhibitors of tubulin polymerization. These conformationally restricted β-lactam structures are not easily isomerized, unlike the *cis*-stilbene **2a**, and are identified as promising lead compounds in the development of new anticancer agents. Further studies are in progress to further rationalize SAR for this series of azetidinones and to determine the antiangiogenic effects of these compounds.

Experimental Section

All reagents were commercially available and were used without further purification unless otherwise indicated. Tetrahydrofuran (THF) was distilled immediately prior to use from Na/benzophenone under a slight positive pressure of nitrogen. Toluene was dried by distillation from sodium and stored on activated molecular sieves (4 Å), and dichloromethane was dried by distillation from calcium hydride prior to use. IR spectra were recorded as thin films on NaCl plates or as KBr discs on a Perkin-Elmer Paragon 100 FT-IR spectrometer. ^{1}H and ^{13}C NMR spectra were obtained on a Bruker Avance DPX 400 instrument at 20 °C, 400.13 MHz for ^{1}H spectra, 100.61 MHz for ^{13}C spectra, in $CDCl_3$, CD_3COCD_3, or CD_3OD (internal standard tetramethylsilane) by Dr. John O'Brien and Dr. Manuel Ruether in the School of Chemistry, Trinity College Dublin. Low resolution mass spectra were run on a Hewlett-Packard 5973 MSD GC−MS system in an electron impact mode, while high resolution accurate mass determinations for all final target compounds were obtained on a Micromass time of flight mass spectrometer (TOF) equipped with electrospray ionization (ES) interface operated in the positive ion mode at the High Resolution Mass Spectrometry Laboratory by Dr. Martin Feeney in the School of Chemistry, Trinity College Dublin. Thin layer chromatography was performed using Merck silica gel 60 TLC aluminum sheets with fluorescent indicator visualizing with UV light at 254 nm. Flash chromatography was carried out using standard silica gel 60 (230−400 mesh) obtained from Merck. All products isolated were homogeneous on TLC. The purity of the tested compounds was determined by HPLC or combustion analysis, and unless otherwise stated, the purity level was ≥95%. Elemental analyses were performed on an Exetor Analytical CE4400 CHN analyzer in the Microanalysis Laboratory, Department of Chemistry, University College Dublin, Ireland. Analytical high-performance liquid chromatography (HPLC) was performed using a Waters 2487 dual wavelength absorbance detector, a Waters 1525 binary HPLC pump, and a Waters 717Plus autosampler. The column used was a Varian Pursuit XRs C18 reverse phase 150 mm × 4.6 mm chromatography column. Samples were detected using a wavelength of 254 nm. All samples were analyzed using acetonitrile (70%)/water (30%) over 10 min and a flow rate of 1 mL/min. Chiral liquid chromatography was carried out on selected compounds using a Chiral-AGP 150 mm × 4.0 mm column supplied by ChromTech Ltd. (now supplied by Chiral Technologies Europe) with a Chiral- AGP guard column. The HPLC system consisted of the following components: a Waters 1525 binary HPLC pump, a Waters 2487 dual wavelength absorbance detector, a Waters in-line degasser AF, and a Waters 717 plus autosampler. Gradient elution was used beginning with 10% of organic phase and finishing with 90% of organic phase over a period of 20 min. The organic mobile phase was 2-propanol, and the aqueous phase was a sodium phosphate buffer. The sodium phosphate buffer, consisting of 10 mM sodium dihydrogen orthophosphate dihydrate (NaH_2PO_4) in HPLC-grade water, was made up to pH 7.0 using sodium hydroxide. The flow rate was 0.5 mL/min, and detection was carried out at 225 nm. Details of the synthesis of intermediate compounds and characterizations of target β-lactams are contained in the Supporting Information.

General Method for Imine Preparation. The appropriate amine (10 mmol) was refluxed with the appropriate aldehyde (10 mmol) in ethanol (50 mL) for 3 h. The reaction mixture was reduced in vacuo, and the resulting solution was allowed to stand until solid product crystallized from solution. The resulting imine was recrystallized from ethanol.

[3-(*tert*-Butyldimethylsilanyloxy)-4-methoxybenzylidene]-(3,4,5-trimethoxyphenyl)amine (5e). 5e was prepared by reacting 3-(*tert*-butyldimethylsilanyloxy)-4-methoxybenzaldehyde with 3,4,5-trimethoxybenzenamine following the general method above. The product was obtained as a yellow solid. Yield 64.3%. Mp 105 °C. IR (KBr) υ 1619.8, 1579.73 cm^{-1} (−C═N−); ^{1}H NMR (400 MHz, $CDCl_3$) δ 0.20 (s, 6H, 2xCH_3), 1.03 (s, 9H, C$(CH_3)_3$), 3.87−3.91 (m, 12H, 4 × OCH_3), 6.48 (s, 2H, ArH), 6.93 (d, 2H, J = 8.04 Hz, ArH), 7.43−7.47 (m, 1H, ArH), 8.35 (s, 1H, CH═N); ^{13}C NMR (100 MHz, $CDCl_3$) δ −5.04 (CH_3−Si−CH_3), 18.03(CH_3−C−CH_3), 25.27 (C$(CH_3)_3$), 54.98 (−OCH_3), 55.63 (−OCH_3), 97.62, 110.94, 119.71, 123.48, 128.95, 135.53, 144.87, 147.94, 153.05, 153.59 (ArC), 158.84 (−C═N−). Elemental analysis: found C, 63.99; H, 7.65; N, 3.21; $C_{23}H_{33}NO_5Si$ requires C, 64.01; H, 7.71; N, 3.25%.

General Method for β-Lactam Synthesis I: Staudinger Reaction (Compounds 7−14). The appropriate imine (5 mmol) and triethylamine (15 mmol) were added to dry CH_2Cl_2 (50 mL), and the mixture was brought to reflux at 60 °C. The appropriate acid chloride (7.5 mmol) was then added dropwise to the mixture via a septum. The reaction mixture was then refluxed for 3 h, then cooled and washed first with distilled water (2 × 50 mL) and then with saturated aqueous sodium bicarbonate solution (50 mL). The organic layer was dried by filtration through anhydrous sodium sulfate. The organic layer containing the product was collected and reduced in vacuo to afford the crude product which was purified by flash column chromatography over silica gel (eluent: hexane/ethyl acetate gradient).

General Method for β-Lactam Synthesis II: Staudinger Reaction Modified (Compounds 15−17). A solution of the appropriate imine (10 mmol) and acid chloride (10 mmol) in CH_2Cl_2 (50 mL) under nitrogen was stirred for 2 h. Triethylamine (10 mmol) was added dropwise, and the mixture was left to stir overnight. The mixture was washed first with distilled water (2 × 50 mL) and then with saturated aqueous sodium bicarbonate solution (50 mL). The organic layer was dried by filtration through anhydrous sodium sulfate. The organic layer containing the product was collected and reduced in vacuo to afford the crude product which was purified by flash column chromatography over silica gel (eluent: hexane/ethyl acetate gradient 10:1 to 2:1).

General Method for β-Lactam Formation III: Acid Activation with Triphosgene (Compounds 18−31). A mixture of the appropriate acetic acid (15 mmol) and triphosgene [bis(trichloromethyl) carbonate] (5 mmol) in dry CH_2Cl_2 (50 mL) was heated at refluxed for 30 min. A solution of the appropriately substituted imine (10 mmol) in dry CH_2Cl_2 (10 mL) was added dropwise to the refluxing solution followed by triethylamine (30 mmol). The reaction mixture was heated at reflux for 5 h and stirred at room temperature overnight. The mixture was washed first with distilled water (2 × 50 mL) and then with saturated aqueous sodium bicarbonate solution (50 mL). The organic layer was dried over anhydrous sodium sulfate to afford the crude product, which was purified by flash column chromatography over silica gel (eluent: hexane/ethyl acetate gradient).

3-(4-(Benzyloxy)phenyl)-4-(3-((*tert*-butyldimethylsilyl)oxy)-4-methoxyphenyl)-1-(3,4,5-trimethoxyphenyl)azetidin-2-one 29. 29 was obtained from (4-benzyloxyphenyl)acetic acid and imine **5e** following general method III as a brown oil, yield 6.8%, and

was deprotected immediately without further purification to afford **37** (see below).

Benzyl (4-(2-(3-((*tert*-Butyldimethylsilyl)oxy)-4-methoxyphenyl)-4-oxo-1-(3,4,5-trimethoxyphenyl)azetidin-3-yl)phenyl)carbamate 30. 30 was obtained from (4-benzyloxycarbonylaminophenyl)acetic acid and imine **5e** following general method III as an oil, yield 10.6%, and was deprotected immediately to afford **38** without further purification.

General Method for β-Lactam Preparation IV: Reformatsky Reaction Using Microwave (Compounds 32−34). Zinc powder (0.927 g, 15 mmol) was activated using trimethylchlorosilane (0.65 mL, 5 mmol) in anhydrous benzene (5 mL) by heating for 15 min at 40 °C and subsequently for 2 min at 100 °C in a microwave. After the mixture was cooled, the appropriately substituted imine (10 mmol) and substituted ethylbromoacetate (12 mmol) were added to the reaction vessel and the mixture was placed in the microwave for 30 min at 100 °C. The reaction mixture was filtered through Celite to remove the zinc catalyst and then diluted with dichloromethane. This solution was washed with saturated ammonium chloride solution (20 mL) and 25% ammonium hydroxide (20 mL) and then with dilute HCl (40 mL) followed by water (40 mL). The organic phase was dried over anhydrous sodium sulfate and the solvent was removed in vacuo to afford the crude product which was purified by flash column chromatography over silica gel (eluent: hexane/ethyl acetate gradient) to afford the required β-lactam product.

4-(4-Methoxyphenyl)-3-phenyl-1-(3,4,5-trimethoxyphenyl)-azetidin-2-one 32. 32 was obtained from ethyl 2-bromo-2-phenylacetate and imine **5a** following general method IV as a white crystalline solid, yield 6.8%. Mp 108 °C. IR (NaCl) υ 1753.3 cm^{-1} (C═O, β-lactam); ^1H NMR (400 MHz, $CDCl_3$) δ 3.72 (s, 6H, 2×-OCH_3), 3.77 (s, 3H, -OCH_3), 3.83 (s, 3H, -OCH_3), 4.29 (d, 1H, J = 2.5 Hz, H-3), 4.87 (d, 1H, J = 2.5 Hz, H-4), 6.60 (s, 2H, ArH), 6.95 (d, 2H, J = 8.5 Hz, ArH), 7.32−7.40 (m, 7H, ArH); ^{13}C NMR (100 MHz, $CDCl_3$) δ 54.92 (−OCH_3), 55.57 (−OCH_3), 60.52 (−OCH_3), 63.40 (C-3), 64.59 (C-4), 94.38, 114.24, 126.89, 127.00, 127.45, 128.59, 128.85, 133.28, 134.00, 134.33, 153.05, 159.49 (ArC), 165.21 (C═O). HRMS calcd for $C_{25}H_{25}NO_5Na$: 442.1630. Found: 442.1631 (M^+ + Na).

4-(3-((*tert*-Butyldimethylsilyl)oxy)-4-methoxyphenyl)-3-phenyl-1-(3,4,5-trimethoxyphenyl)azetidin-2-one 34. 34 was obtained from ethyl 2-bromo-2-phenylacetate and imine **5e** following general method IV as a yellow oil, yield 70%, and was immediately deprotected to form **35** without further purification.

Desilylation of β-Lactams (General Method V) (Compounds 35−38). To a solution of the appropriately protected phenol (10 mmol) in THF (50 mL) was added 1 M tetrabutylammonium fluoride (1.5 equiv). The solution was stirred in an ice bath for 15 min. The reaction mixture was diluted with EtOAc (100 mL) and quenched with HCl (10%, 100 mL). The layers were separated, and the aqueous layer was extracted with EtOAc (2 × 50 mL). The organic layer was then washed with water (100 mL) and brine (100 mL), followed by drying over anhydrous sodium sulfate. The solvent was removed by evaporation under reduced pressure and the crude product was purified by flash column chromatography over silica gel (eluent: hexane/ethyl acetate gradient) to afford the required phenol product.

4-(3-Hydroxy-4-methoxyphenyl)-3-phenyl-1-(3,4,5-trimethoxyphenyl)azetidin-2-one 35. 35 was obtained from azetidinone **34** following general method V as a white solid, yield 97.3%. Mp 110 °C. IR (KBr) υ 1718.2 cm^{-1} (C═O, β-lactam); ^1H NMR (400 MHz, $CDCl_3$) δ 3.73 (s, 6H, 2×-OCH_3), 3.78 (s, 3H, OCH_3), 3.91 (s, 3H, OCH_3), 4.27 (d, 1H, J = 2.5 Hz, H-3), 4.81 (d, 1H, J = 2.5 Hz, H-4), 5.75 (s, 1H, OH), 6.63 (s, 2H, ArH), 6.86−6.93 (m, 2H, ArH), 7.00 (d, 1H, J = 2.0 Hz, ArH), 7.31−7.39 (m, 5H, ArH); ^{13}C NMR (100 MHz, $CDCl_3$) δ 55.58-(OCH_3), 55.60(OCH_3), 60.51(OCH_3), 63.36(H-3), 64.49(H-4), 94.42, 110.59, 111.56, 117.40, 126.97, 127.43, 128.57, 130.10, 133.27, 134.02, 134.31, 145.91, 146.43, 153.05(ArC), 165.14(C═O). HRMS calcd for $C_{25}H_{25}NO_6Na$:458.1580. Found: 458.1575 (M^+ + Na).

3-(4-(Benzyloxy)phenyl)-4-(3-hydroxy-4-methoxyphenyl)-1-(3,4,5-trimethoxyphenyl)azetidin-2-one 37. 37 was obtained from azetidinone **29** following general method V as a brown oil, yield 96.8%, which was further deprotected to form **41** without purification.

{4-[2-(3-Hydroxy-4-methoxyphenyl)-4-oxo-1-(3,4,5-trimethoxyphenyl)-azetidin-3-yl]phenyl}carbamic Acid Benzyl Ester 38. 38 was obtained from carbamate **30** following general method V, yield 33.7%, and was further deprotected to **46** without purification.

Debenzylation of β-Lactams (General Method VI) (Compounds 39−42). The appropriate benzyl ether compound (2 mmol) was dissolved in ethanol/ethyl acetate (50 mL, 1:1 mixture) and hydrogenated over palladium on carbon (1.2 g, 10%) at atmospheric pressure for 2 h. The catalyst was filtered, the solvent was removed under vacuum, and the product was purified by flash column chromatography over silica gel (eluent: hexane/ethyl acetate gradient) to afford the phenolic product.

4-(3-Hydroxy-4-methoxyphenyl)-3-(4-hydroxyphenyl)-1-(3,4,5-trimethoxyphenyl)azetidin-2-one 41. 41 was obtained from azetidinone **37** following general method VI as a white powder, yield 2.9%. Mp 152 °C. IR (NaCl film) υ 1720.6 cm^{-1} (C═O, β-lactam); ^1H NMR (400 MHz, $CDCl_3$) δ 3.65 (s, 3H, -OCH_3), 3.70 (s, 6H, 2×-OCH_3), 3.86 (s, 3H, −OCH_3), 4.26 (d, 1H, J = 2.4 Hz, H-3), 4.98 (d, 1H, J = 2.4 Hz, H-4), 6.71 (s, 2H, ArH), 6.87 (d, 2H, J = 8.8 Hz, ArH), 7.00 (s, 3H, ArH), 7.22 (d, 2H, J = 8.8 Hz, ArH); ^{13}C NMR (100 MHz, $CDCl_3$) δ 54.93 (−OCH_3), 59.23 (−OCH_3), 63.05 (C-3), 63.76 (C-4), 94.66, 111.31, 112.22, 115.13, 117.48, 125.72, 128.25, 130.39, 133.49, 134.12, 146.70, 147.32, 153.25, 156.50 (ArC), 165.27 (C═O). HRMS calcd for $C_{25}H_{25}NO_7Na$: 474.1529. Found 474.1548; (M^+ + Na).

General Method for Reduction of Nitro-Substituted Azetidinones (General Method VII) (Compounds 43−45). To the appropriate nitro substituted β-lactam (10 mmol) dissolved in the minimum amount of glacial AcOH (2−3 mL) was added metallic zinc dust (10 equiv). The mixture was stirred for 6 days at room temperature under nitrogen. The residue was filtered through Celite and was extracted with dichloromethane. The solvent was evaporated and the residue purified by flash column chromatography over silica gel (eluent: hexane/ethyl acetate gradient) to afford the required amine product.

Deprotection of the Cbz Protected Azetidinones (General Method VIII) (Compounds 46 and 47). The Cbz-protected compound (2 mmol) was dissolved in ethanol/ethyl acetate (50 mL; 1:1 mixture) and hydrogenated over palladium on carbon (1.2 g, 10%) for 2 h. The catalyst was filtered, the solvent was removed under vacuum, and the product was purified by flash column chromatography over silica gel (eluent: hexane/ethyl acetate gradient) to afford the amine product.

3-(4-Aminophenyl)-4-(3-hydroxy-4-methoxyphenyl)-1-(3,4,5-trimethoxyphenyl)azetidin-2-one 46. 46 was obtained from carbamate **38** following general method VIII, as an orange oil, yield 39.4%. IR (NaCl film) υ 1737.4 cm^{-1} (C═O, β-lactam); ^1H NMR (400 MHz, $CDCl_3$) δ 3.75 (s, 6H, 2×-OCH_3), 3.80 (s, 3H, −OCH_3), 3.93 (s, 3H, -OCH_3), 4.18 (d, 1H, J = 2.5 Hz, H-3), 4.74 (d, 1H, J = 2.5 Hz, H-4), 6.63 (s, 2H, ArH), 6.70 (d, 2H, J = 8.3 Hz, ArH), 6.89 (m, 2H, ArH), 6.99 (s, 1H, ArH), 7.11 (d, 2H, J = 8.3 Hz, ArH); ^{13}C NMR (100 MHz, $CDCl_3$) δ 55.56 (−OCH_3), 55.59 (−OCH_3), 60.51 (−OCH_3), 63.85 (C-3), 64.19 (C-4), 94.39, 110.54, 111.53, 115.15, 117.33, 124.24, 128.03, 130.32, 133.39, 145.39, 145.8, 146.32, 153.02(ArC), 165.60 (−C═O). HRMS calcd for $C_{25}H_{27}N_2O_6$: 451.1869. Found: 451.1859 (M^+).

Antiproliferative MTT Assay. All assays were performed in triplicate for the determination of mean values reported. Compounds were assayed as the free bases isolated from reaction. The human breast tumor cell line MCF-7 was cultured in Eagles minimum essential medium in a 95% O_2/5% CO_2 atmosphere with 10% fetal bovine serum, 2 mM L-glutamine, and 100 μg/mL penicillin/streptomycin. The medium was supplemented with 1% nonessential amino acids. MDA-MB-231 cells were maintained in Dulbecco's modified Eagle's medium (DMEM), supplemented

with 10% (v/v) fetal bovine serum, 2 mM L-glutamine, and 100 μg/mL penicillin/streptomycin (complete medium). Cells were trypsinized and seeded at a density of 2.5×10^4 cells/mL in a 96-well plate and incubated at 37 °C in 95%O_2/5% CO_2 atmosphere for 24 h. After this time they were treated with 2 μL volumes of test compound which had been preprepared as stock solutions in ethanol to furnish the concentration range of study, 1 nM to 100 μM, and reincubated for a further 72 h. Control wells contained the equivalent volume of the vehicle ethanol (1% v/v). The culture medium was then removed. The cells were washed with 100 μL of phosphate buffered saline (PBS), and 50 μL MTT was added to reach a final concentration of 1 mg/mL MTT. Cells were incubated for 2 h in darkness at 37 °C. At this point solubilization was begun through the addition of 200 μL of DMSO and the cells were maintained at room temperature in darkness for 20 min to ensure thorough color diffusion before reading the absorbance. The absorbance value of control cells (no added compound) was set to 100% cell viability, and from this graphs of absorbance versus cell density per well were prepared to assess cell viability using GraphPad Prism software.

Cytotoxicity Assay. Mammary glands from 14 to 18 day pregnant CD-1 mice were used as source, and primary mammary epithelial cell cultures were prepared from these. The first to third thoracic glands were exposed by pulling the skin back from the rib cage to the forelimb and extracted in a similar way to the inguinal glands. Midpregnant glands are large, soft, and pink in color. Mammary glands that were spongy and pale in color were not used, as these glands had matured and were producing milk. The harvested glands were then subjected to mechanical and enzymatic digestion to release immature alveolar structures and isolate mammary epithelial cells. The dissected glands were weighed, and fresh collagenase digestion mixture was prepared. It contained 480 mg of F10 powdered medium (Sigma), 70 mg of trypsin (GibcoBrl, Life Technologies), 150 mg of collagenase A (GibcoBrl, Life Technologies), and 2.5 mL of fetal calf serum (GibcoBrl, Life Technologies) in a final volume of 50 mL (with sterile water). The collagenase digestion mixture was subsequently adjusted to pH 7.4, filtered through a 0.2 μM sterile filter, and stored at 4 °C until required. The dissected glands were minced criss-cross using two sterile scalpel blades. The minced glands were placed in an autoclaved, sterile 250 mL glass conical flask with the collagenase digestion mixture (~4 mL of digestion mixture per gram of tissue) and digested for 90 min on a shaking table, 250 rpm at 37 °C. After this step, a stringent washing/centrifugation protocol was used to isolate epithelial cells from fibroblasts. Selective centrifugation was carried out as follows: the digested cell suspension was removed to a 50 mL tube and centrifuged for 30 s at 100 rpm The supernatant was transferred to a fresh tube and centrifuged at 800 rpm for 3 min. The pellet was then subjected to a DNase treatment in order to achieve separation of single epithelial cells rather than cell clumps. The DNase mixture contained 480 mg of F10 powdered medium (Sigma), 250 μL of 10 mg/mL DNase (Roche Diagnostics), and 250 μL of 1 M $MgCl_2$ brought up to a final volume of 50 mL (with water) and passed through a 0.2 μM sterile filter. The pellet was resuspended in the DNase mixture and incubated at 37 °C for 30 min on a shaking table at 150 rpm The cell suspension was then transferred to a fresh 50 mL tube and centrifuged at 800 rpm for 3 min. The supernatant was discarded. The pellet was resuspended in 30−50 mL of Ham's F-12 medium (with gentamycin, Biowhittaker), depending on the size of the pellet. Finally, the cell suspension was added to F-12 medium containing gentamycin (50 μg/mL) with the following: hydrocortisone (H) 1 μg/mL (Sigma, stock solution, 1 mg/mL in 100% ethanol), insulin (I) 5 μg/mL (Sigma, stock solution, 5 mg/mL in 5 mM HCl), and epidermal growth factor (EGF) 5 ng/mL (Promega, stock solution, 5 μg/mL in F-12 medium). The isolated mammary epithelial cells were seeded at two concentrations (25 000 cells/mL and 50 000 cells/mL). Initially a third concentration of 100 000 cells/mL was also used, but this proved to be too high to give meaningful results. After 24 h, they were treated with 2 μL volumes of test compound which had been preprepared as stock solutions in ethanol to furnish the concentration range of study, 1 nM to 100 μM, and reincubated for a further 72 h. Control wells contained the equivalent volume of the vehicle ethanol (1% v/v). The cytotoxicity was assessed using alamarBlue dye.

Tubulin Polymerization. Tubulin polymerization was carried out using a kit supplied by Cytoskeleton. It is based on the principal that light is scattered by microtubules to an extent that is proportional to the concentration of the microtubule polymer. Compounds that interact with tubulin will alter the polymerization of tubulin, and this can be detected using a spectrophotometer. The absorbance at 340 nm at 37 °C is monitored. The experimental procedure of the assay was performed as described in version 8.2 of the tubulin polymerization assay kit manual.[68]

Stability Study for Compounds 32 and 35. Analytical high-performance liquid chromatography (HPLC) stability studies were performed using a Symmetry column (C_{18}, 5 μm, 4.6 mm × 150 mm), a Waters 2487 dual wavelength absorbance detector, a Waters 1525 binary HPLC pump, and a Waters 717plus autosampler. Samples were detected at a wavelength of 254 nm. All samples were analyzed using acetonitrile (80%)/water (20%) as the mobile phase over 10 min and a flow rate of 1 mL/min. Stock solutions are prepared by dissolving 5 mg of compound in 10 mL of mobile phase. Phosphate buffers at the desired pH values (4, 7.4, and 9) were prepared in accordance with the British Pharmacopoeia monograph 2010. Then 30 μL of stock solution was diluted with 1 mL of appropriate buffer, shaken, and injected immediately. Samples were withdrawn and analyzed at time intervals of $t = 0$ min, 5 min, 30 min, 60 min, 90 min, 120 min, and 21 h.

Computational Procedure. For ligand preparation, all compounds were built using ACD/Chemsketch, version 10, to generate SMILES. A single conformer from each string was generated using Corina, version 3.4, and ensuring that Omega, version 2.2.1, was subsequently employed to generate a maximum of 1000 conformations of each compound. For the receptor preparation, the PDB entry 1SA0 was downloaded from the Protein Data Bank (PDB). All waters were retained in both isoforms. Addition and optimization of hydrogen positions for these waters were carried out using MOE 2007.09, ensuring all other atom positions remained fixed. By use of the reported X-ray structure of tubulin cocrystallized with a colchicine derivative, DAMA-colchicine (PDB entry 1SA0),[63] possible binding orientations ligands were probed with the docking program FRED, version 2.2.3 (Openeye Scientific Software).[64] Docking was carried out using FRED, version 2.2.3, in conjunction with Chemgauss3 PLP scoring function. The 3D ligand conformations were enumerated using CORINA, version 3.4 (Molecular Networks GMBH),[69] for ligands followed by generation of multiple conformations using OMEGA, version2.2.1 (Openeye Scientific Software).[70] Each conformation was subsequently docked and scored with Chemgauss3 PLP as outlined previously.[32] The top binding poses were refined using the LigX procedure (MOE, Chemical Computing Group)[71] together with Postdock analysis (SVL script, MOE) of the docked ligand poses.

X-ray Crystallography. The X-ray crystallography data for crystal **32** were collected on a Rigaku Saturn 724 CCD diffractometer. A suitable crystal was selected and mounted on a glass fiber tip and placed on the goniometer head in a 123K N2 gas stream. The data set was collected using Crystalclear-SM 1.4.0 software, and 1680 diffraction images of 0.5° per image were recorded. Data integration, reduction, and correction for absorption and polarization effects were all performed using Crystalclear-SM 1.4.0 software. Space group determination, structure solution, and refinement were obtained using Crystalstructure, version 3.8, and Bruker Shelxtl, version 6.14, software.[72] Crystal data for **32** are as follows: $C_{25}H_{25}NO_5$, MW 419.46, orthorhombic,

space group *Pbca*, a = 18.876(9) Å, b = 9.608(5) Å, c = 23.662(12) Å, $\alpha = \beta = \gamma = 90°$, U = 4291(4) Å, $Z = 8$, $D_c = 1.298$ Mg m^{-3}, m = 0.090 mm^{-1}, range for data collection = 1.12−25.00, reflections collected 17 904, unique reflections 3777 [R_{int} = 0.1746], data/restraints/parameters 3777/0/284, goodness-of-fit on F^2 1.357, R indices (all data) = R1 = 0.1908, wR2 = 0.2609, final R indices [$I > 2\sigma(I)$] = R1 = 0.2366, wR2 = 0.2809, CCDC deposition no. 775568.

Acknowledgment. We thank Dr. Niall Keely for the kind gift of combretastatin A-4. This work was supported through funding from the Trinity College Dublin IITAC research initiative (HEA PRTLI), Enterprise Ireland (EI), Science Foundation Ireland (SFI), and the Health Research Board (HRB), with additional support for computational facilities from the Wellcome Trust. A postgraduate research award from Trinity College Dublin is gratefully acknowledged.

Supporting Information Available: Experimental procedures and spectroscopic data for intermediate and final compounds, additional cytotoxicity data in normal murine epithelial cells for compounds **35** and **41**, results of comparative antitumor evaluations of compounds **9** and **35** in the NCI60 cell line in vitro primary screen, and results of standard COMPARE analysis of **35**. This material is available free of charge via the Internet at http://pubs.acs.org.

References

(1) Downing, K. H.; Nogales, E. Tubulin and microtubule structure. *Curr. Opin. Cell Biol.* **1998**, *10* (1), 16–22.
(2) Jordan, M. A. Mechanism of action of antitumor drugs that interact with microtubules and tubulin. *Curr. Med. Chem.: Anti-Cancer Agents* **2002**, *2* (1), 1–17.
(3) Bhattacharyya, B.; Panda, D.; Gupta, S.; Banerjee, M. Anti-mitotic activity of colchicine and the structural basis for its interaction with tubulin. *Med. Res. Rev.* **2008**, *28* (1), 155–183.
(4) Margolis, R. L.; Rauch, C. T.; Wilson, L. Mechanism of colchicine-dimer addition to microtubule ends: implications for the microtubule polymerization mechanism. *Biochemistry* **1980**, *19* (24), 5550–5557.
(5) Hadfield, J. A.; Ducki, S.; Hirst, N.; McGown, A. T. Tubulin and microtubules as targets for anticancer drugs. *Prog. Cell Cycle Res.* **2003**, *5*, 309–325.
(6) Jordan, M. A.; Wilson, L. Microtubules as a target for anticancer drugs. *Nat. Rev. Cancer* **2004**, *4* (4), 253–265.
(7) Dark, G. G.; Hill, S. A.; Prise, V. E.; Tozer, G. M.; Pettit, G. R.; Chaplin, D. J. Combretastatin A-4, an agent that displays potent and selective toxicity toward tumor vasculature. *Cancer Res.* **1997**, *57* (10), 1829–1834.
(8) Pandit, B.; Sun, Y.; Chen, P.; Sackett, D. L.; Hu, Z.; Rich, W.; Li, C.; Lewis, A.; Schaefer, K.; Li, P.-K. Structure−activity-relationship studies of conformationally restricted analogs of combretastatin A-4 derived from SU5416. *Bioorg. Med. Chem.* **2006**, *14* (19), 6492–6501.
(9) Watt, J. M.; Gerdina, M. *The Medicinal and Poisonous Plants of Southern and Eastern Africa*; E. & S. Livingstone Ltd.: Edinburgh and London, U.K., 1962.
(10) Cragg, G. M., Kingston, D. G., Newman, D. J. *Anticancer Agents from Natural Products* CRC Press: Boca Raton, FL, 2005.
(11) Cooney, M. M.; Ortiz, J.; Bukowski, R. M.; Remick, S. C. Novel vascular targeting/disrupting agents: combretastatin A4 phosphate and related compounds. *Curr. Oncol. Rep.* **2005**, *7* (2), 90–95.
(12) Young, S. L.; Chaplin, D. J. Combretastatin A4 phosphate: background and current clinical status. *Expert Opin. Invest. Drugs* **2004**, *13* (9), 1171–1182.
(13) http://www.clinicaltrials.gov/ct/gui/show/NCT00060242.
(14) Rustin, G. J.; Shreeves, G.; Nathan, P. D.; Gaya, A.; Ganesan, T. S.; Wang, D.; Boxall, J.; Poupard, L.; Chaplin, D. J.; Stratford, M. R.; Balkissoon, J.; Zweifel, M. A phase Ib trial of CA4P (combretastatin A-4 phosphate), carboplatin, and paclitaxel in patients with advanced cancer. *Br. J. Cancer* **2010**, *102*, 1355–1360.
(15) Cirla, A.; Mann, J. Combretastatins: from natural products to drug discovery. *Nat. Prod. Rep.* **2003**, *20* (6), 558–564.
(16) Bohle, A. S.; Leuschner, I.; Kalthoff, H.; Henne-Bruns, D. Combretastatin A-4 prodrug: a potent inhibitor of malignant hemangioendothelioma cell proliferation. *Int. J. Cancer* **2000**, *87* (6), 838–843.
(17) Ohsumi, K.; Hatanaka, T.; Nakagawa, R.; Fukuda, Y.; Morinaga, Y.; Suga, Y.; Nihei, Y.; Ohishi, K.; Akiyama, Y.; Tsuji, T. Synthesis and antitumor activities of amino acid prodrugs of amino-combretastatins. *Anti-Cancer Drug Design* **1999**, *14*, 539–548.
(18) Kanthou, C.; Tozer, G. M. Microtubule depolymerizing vascular disrupting agents: novel therapeutic agents for oncology and other pathologies. *Int. J. Exp. Pathol.* **2009**, *90* (3), 284–294.
(19) Hinnen, P.; Eskens, F. A. L. M. Vascular disrupting agents in clinical development. *Br. J. Cancer* **2007**, *96* (8), 1159–1165.
(20) Lippert, J. W. Vascular disrupting agents. *Bioorg. Med. Chem.* **2007**, *15* (2), 605–615.
(21) Pinney, K. G.; Mejia, M. P.; Villalobos, V. M.; Rosenquist, B. E.; Pettit, G. R.; Verdier-Pinard, P.; Hamel, E. Synthesis and biological evaluation of aryl azide derivatives of combretastatin a-4 as molecular probes for tubulin. *Bioorg. Med. Chem.* **2000**, *8* (10), 2417–2425.
(22) Pettit, G. R.; Rhodes, M. R.; Herald, D. L.; Hamel, E.; Schmidt, J. M.; Pettit, R. K. Antineoplastic agents. 445. Synthesis and evaluation of structural modifications of (*Z*)- and (*E*)-combretastatin A-41. *J. Med. Chem.* **2005**, *48* (12), 4087–4099.
(23) Ohsumi, K.; Hatanaka, T.; Fujita, K.; Nakagawa, R.; Fukuda, Y.; Nihei, Y.; Suga, Y.; Morinaga, Y.; Akiyama, Y.; Tsuji, T. Syntheses and antitumor activity of cis-restricted combretastatins: 5-membered heterocyclic analogues. *Bioorg. Med. Chem. Lett.* **1998**, *8* (22), 3153–3158.
(24) Cushman, M.; He, H. M.; Lin, C. M.; Hamel, E. Synthesis and evaluation of a series of benzylaniline hydrochlorides as potential cytotoxic and antimitotic agents acting by inhibition of tubulin polymerization. *J. Med. Chem.* **1993**, *36* (19), 2817–2821.
(25) Tron, G. C.; Pirali, T.; Sorba, G.; Pagliai, F.; Busacca, S.; Genazzani, A. A. Medicinal chemistry of combretastatin A4: present and future directions. *J. Med. Chem.* **2006**, *49* (11), 3033–3044.
(26) Nam, N. H. Combretastatin A-4 analogues as antimitotic antitumor agents. *Curr. Med. Chem.* **2003**, *10* (17), 1697–1722.
(27) Liou, J. P.; Chang, Y. L.; Kuo, F. M.; Chang, C. W.; Tseng, H. Y.; Wang, C. C.; Yang, Y. N.; Chang, J. Y.; Lee, S. J.; Hsieh, H. P. Concise synthesis and structure−activity relationships of combretastatin A-4 analogues, 1-aroylindoles and 3-aroylindoles, as novel classes of potent antitubulin agents. *J. Med. Chem.* **2004**, *47* (17), 4247–4257.
(28) Ohsumi, K.; Nakagawa, R.; Fukuda, Y.; Hatanaka, T.; Morinaga, Y.; Nihei, Y.; Ohishi, K.; Suga, Y.; Akiyama, Y.; Tsuji, T. Novel combretastatin analogues effective against murine solid tumors: design and structure−activity relationships. *J. Med. Chem.* **1998**, *41* (16), 3022–3032.
(29) Ganina, O. G.; Daras, E.; Bourgarel-Rey, V.; Peyrot, V.; Andresyuk, A. N.; Finet, J. P.; Fedorov, A. Y.; Beletskaya, I. P.; Combes, S. Synthesis and biological evaluation of polymethoxylated 4-hetero-arylcoumarins as tubulin assembly inhibitor. *Bioorg. Med. Chem.* **2008**, *16* (19), 8806–8812.
(30) Wang, L.; Woods, K. W.; Li, Q.; Barr, K. J.; McCroskey, R. W.; Hannick, S. M.; Gherke, L.; Credo, R. B.; Hui, Y. H.; Marsh, K.; Warner, R.; Lee, J. Y.; Zielinski-Mozng, N.; Frost, D.; Rosenberg, S. H.; Sham, H. L. Potent, orally active heterocycle-based combretastatin A-4 analogues: synthesis, structure-activity relationship, pharmacokinetics, and in vivo antitumor activity evaluation. *J. Med. Chem.* **2002**, *45*, 1697–1711.
(31) Shirai, R.; Takayama, H.; Nishikawa, A.; Koiso, Y.; Hashimoto, Y. Asymmetric synthesis of antimitotic combretadioxolane with potent antitumor activity against multi-drug resistant cells. *Bioorg. Med. Chem. Lett.* **1998**, *8* (15), 1997–2000.
(32) Barrett, I.; Carr, M.; O'Boyle, N.; Greene, L. M.; Knox, A., J. S.; Lloyd, D. G.; Zisterer, D. M.; Meegan, M. J. Lead identification of conformationally restricted benzoxepin type combretastatin analogs: synthesis, antiproliferative activity, and tubulin effects. *J. Enzyme Inhib. Med. Chem.* **2010**, *25* (2), 180–194.
(33) Banik, I.; Becker, F. F.; Banik, B. K. Stereoselective synthesis of beta-lactams with polyaromatic imines: entry to new and novel anticancer agents. *J. Med. Chem.* **2003**, *46* (1), 12–15.
(34) Sun, L.; Vasilevich, N. I.; Fuselier, J. A.; Hocart, S. J.; Coy, D. H. Examination of the 1,4-disubstituted azetidinone ring system as a template for combretastatin A-4 conformationally restricted analogue design. *Bioorg. Med. Chem. Lett.* **2004**, *14* (9), 2041–2046.
(35) Carr, M.; Greene, L. M.; Knox, A. J. S.; Lloyd, D. G.; Zisterer, D. M.; Meegan, M. J. Lead identification of conformationally restricted [beta]-lactam type combretastatin analogues: synthesis, antiproliferative activity and tubulin targeting effects. *Eur. J. Med. Chem.* **2010**, doi:10.1016/j.ejmech.2010.09.033.
(36) Meegan, M. J.; Carr, M.; Knox, A. J.; Zisterer, D. M.; Lloyd, D. G. Beta-lactam type molecular scaffolds for antiproliferative activity: synthesis and cytotoxic effects in breast cancer cells. *J. Enzyme Inhib. Med. Chem.* **2008**, *23* (5), 668–685.

(37) Banik, B. K.; Banik, I.; Becker, F. F. Stereocontrolled synthesis of anticancer [beta]-lactams via the Staudinger reaction. *Bioorg. Med. Chem.* **2005**, *13* (11), 3611–3622.
(38) Pettit, G. R.; Smith, C. R.; Singh, S. B. *Recent Advances in the Chemistry of Plant Antineoplastic Constituents*; Oxford University Press: Oxford, U.K., 1987.
(39) Wuts, P. G. M.; Greene, T. W. *Greene's Protective Groups in Organic Synthesis*, 4th ed.; John Wiley & Sons, Inc.: Hoboken, NJ, 2007.
(40) Rapson, W. S.; Robinson, R. Synthesis of substances related to the sterols. VII. *J. Chem. Soc.* **1935**, 1533–1543.
(41) Langenbeck, W.; Augustin, M.; Buege, A. Preparation of peptides of *p*-aminophenylacetic acid. *J. Prakt. Chem.* (*Leipzig*) **1965**, *27* (1−2), 57–63.
(42) Bose, A. K.; Spiegelman, G.; Manhas, M. S. Studies on lactams. Part XVI. Stereochemistry of *β*-lactam formation. *Tetrahedron Lett.* **1971**, *12* (34), 3167–3170.
(43) Singh, G. S. Recent progress in the synthesis and chemistry of azetidinones. *Tetrahedron* **2003**, *59* (39), 7631–7649.
(44) Krishnaswamy, D.; Govande, V. V.; Gumaste, V. K.; Bhawal, B. M.; Deshmukh, A. R. A. S. Triphosgene: a versatile reagent for the synthesis of azetidin-2-ones. *Tetrahedron* **2002**, *58* (11), 2215–2225.
(45) Ocampo, R.; Dolbier, J. W. R. The Reformatsky reaction in organic synthesis. Recent advances. *Tetrahedron* **2004**, *60* (42), 9325–9374.
(46) Palomo, C.; Cossio, F. P.; Arrieta, A.; Odriozola, J. M.; Oiarbide, M.; Ontoria, J. M. The Reformatsky type reaction of Gilman and Speeter in the preparation of valuable beta-lactams in carbapenem synthesis: scope and synthetic utility. *J. Org. Chem.* **1989**, *54* (24), 5736–5745.
(47) Picotin, G.; Miginiac, P. Activation of zinc by trimethylchlorosilane. An improved procedure for the preparation of .beta.-hydroxy esters from ethyl bromoacetate and aldehydes or ketones (Reformatsky reaction). *J. Org. Chem.* **1987**, *52* (21), 4796–4798.
(48) D'hooghe, M.; Dekeukeleire, S.; Mollet, K.; Lategan, C.; Smith, P. J.; Chibale, K.; De Kimpe, N. Synthesis of novel 2-alkoxy-3-amino-3-arylpropan-1-ols and 5-alkoxy-4-aryl-1,3-oxazinanes with antimalarial activity. *J. Med. Chem.* **2009**, *52* (13), 4058–4062.
(49) Moyna, G.; Williams, H. J.; Scott, A. I. Preparation of aminated Taxol side chain precursors. A simple approach to 2,3-diamond acids using the beta-lactam synthon method. *Synth. Commun.* **1997**, *27* (9), 1561–1567.
(50) Klein, S. I.; Czekaj, M.; Gardner, C. J.; Guertin, K. R.; Cheney, D. L.; Spada, A. P.; Bolton, S. A.; Brown, K.; Colussi, D.; Heran, C. L.; Morgan, S. R.; Leadley, R. J.; Dunwiddie, C. T.; Perrone, M. H.; Chu, V. Identification and initial structure−activity relationships of a novel class of nonpeptide inhibitors of blood coagulation factor Xa. *J. Med. Chem.* **1998**, *41* (4), 437–450.
(51) De Vitis, L.; Troisi, L.; Granito, C.; Pindinelli, E.; Ronzini, L. Tandem-selective bond cleavage of the lactam nucleus and Michael reaction. *Eur. J. Org. Chem.* **2007**, *2007* (2), 356–362.
(52) Anand, A.; Bhargava, G.; Hundal, M. S.; Mahajan, M. P. A facile sodium alkoxide mediated ring opening of unactivated alpha-dienyl-beta-lactams: synthesis of unnatural multicomponent beta-aminodienoic esters. *Heterocycles* **2007**, *73*, 689–698.
(53) Miller, R. E.; Nord, F. F. Studies on the chemistry of heterocyclics. XVII. Thiophene polyene acids, aldehydes, and ketones. *J. Org. Chem.* **2002**, *16* (11), 1720–1730.
(54) http://dtp.cancer.gov (accessed May 11, 2010).
(55) Paull, K. D.; Shoemaker, R. H.; Hodes, L.; Monks, A.; Scudiero, D. A.; Rubinstein, L.; Plowman, J.; Boyd, M. R. Display and analysis of patterns of differential activity of drugs against human tumor cell lines: development of mean graph and COMPARE algorithm. *J. Natl. Cancer. Inst.* **1989**, *81*, 1088–1092.
(56) DTP Human Tumour Cell Line Screen Standard Agent Database. http://dtp.nci.nih.gov/docs/cancer/searches/standard_agent.html (accessed May 11, 2009).
(57) Paull, K. D.; Lin, C. M.; Malspeis, L.; Hamel, E. Identification of novel antimitotic agents acting at the tubulin level by computer-assisted evaluation of differential cytotoxicity data. *Cancer Res.* **1992**, *52*, 3892–3900.
(58) Furlong, E. E.; Keon, N. K.; Thornton, F. D.; Rein, T.; Martin, F. Expression of a 74-kDa nuclear factor 1 (NF1) protein is induced in mouse mammary gland involution. Involution-enhanced occupation of a twin NF1 binding element in the testosterone-repressed prostate message-2/clusterin promoter. *J. Biol. Chem.* **1996**, *271* (47), 29688–29697.
(59) Murtagh, J.; McArdle, E.; Gilligan, E.; Thornton, L.; Furlong, F.; Martin, F. Organization of mammary epithelial cells into 3D acinar structures requires glucocorticoid and JNK signaling. *J. Cell Biol.* **2004**, *166* (1), 133–143.
(60) Simoni, D.; Romagnoli, R.; Baruchello, R.; Rondanin, R.; Rizzi, M.; Pavani, M. G.; Alloatti, D.; Giannini, G.; Marcellini, M.; Riccioni, T.; Castorina, M.; Guglielmi, M. B.; Bucci, F.; Carminati, P.; Pisano, C. Novel combretastatin analogues endowed with antitumor activity. *J. Med. Chem.* **2006**, *49* (11), 3143–3152.
(61) Gastpar, R.; Goldbrunner, M.; Marko, D.; von Angerer, E. Methoxy-substituted 3-formyl-2-phenylindoles inhibit tubulin polymerization. *J. Med. Chem.* **1998**, *41* (25), 4965–4972.
(62) Lara-Ochoa, F.; Espinosa-Pérez, G. A new synthesis of combretastatins A-4 and AVE-8062A. *Tetrahedron Lett.* **2007**, *48* (39), 7007–7010.
(63) Ravelli, R. B.; Gigant, B.; Curmi, P. A.; Jourdain, I.; Lachkar, S.; Sobel, A.; Knossow, M. Insight into tubulin regulation from a complex with colchicine and a stathmin-like domain. *Nature* **2004**, *428* (6979), 198–202.
(64) Schulz-Gasch, T.; Stahl, M. Binding site characteristics in structure-based virtual screening: evaluation of current docking tools. *J. Mol. Model.* **2003**, *9* (1), 47–57.
(65) Nguyen, T. L.; McGrath, C.; Hermone, A. R.; Burnett, J. C.; Zaharevitz, D. W.; Day, B. W.; Wipf, P.; Hamel, E.; Gussio, R. A common pharmacophore for a diverse set of colchicine site inhibitors using a structure-based approach. *J. Med. Chem.* **2005**, *48* (19), 6107–6116.
(66) La Regina, G.; Sarkar, T.; Bai, R.; Edler, M. C.; Saletti, R.; Coluccia, A.; Piscitelli, F.; Minelli, L.; Gatti, V.; Mazzoccoli, C.; Palermo, V.; Mazzoni, C.; Falcone, C.; Scovassi, A. I.; Giansanti, V.; Campiglia, P.; Porta, A.; Maresca, B.; Hamel, E.; Brancale, A.; Novellino, E.; Silvestri, R. New arylthioindoles and related bioisosteres at the sulfur bridging group. 4. Synthesis, tubulin polymerization, cell growth inhibition, and molecular modeling studies. *J. Med. Chem.* **2009**, *52* (23), 7512–7527.
(67) Clark, A. M.; Labute, P. 2D depiction of protein−ligand complexes. *J. Chem. Inf. Model.* **2007**, *47* (5), 1933–1944.
(68) *Tubulin Polymerization Assay Kit Manual* (*CDS03 and BK006*); Cytoskeleton: Denver, CO, 2009; pp 1−18.
(69) *CORINA v3.4: www.molecular-networks.com*, Molecular Networks GmbH: Erlangen, Germany, 2010.
(70) *OMEGA v2.2.1: www.eyesopen.com*, Openeye Scientific Software: Santa Fe, New Mexico, 2010.
(71) *MOE*, version 2008.10; Chemical Computing Group: Montreal, Canada; http://www.chemcomp.com.
(72) Sheldrick, G. M. *SHELXTL, An Integrated System for Data Collection, Processing, Structure Solution and Refinement. Software Reference Manual*; Bruker AXS, Inc.: Madison, WI, 2001.
(73) Flynn, B. L.; Flynn, G. P.; Hamel, E.; Jung, M. K. The synthesis and tubulin binding activity of thiophene-based analogues of combretastatin A-4. *Bioorg. Med. Chem. Lett.* **2001**, *11* (17), 2341–2343.
(74) De Martino, G.; La Regina, G.; Coluccia, A.; Edler, M. C.; Barbera, M. C.; Brancale, A.; Wilcox, E.; Hamel, E.; Artico, M.; Silvestri, R. Arylthioindoles, potent inhibitors of tubulin polymerization. *J. Med. Chem.* **2004**, *47* (25), 6120–6123.